UNIVERSITY of SOPRON | FACULTY OF FORESTRY

INSTITUTE OF ENVIRONMENTAL PROTECTION AND NATURE CONSERVATION

MASTER THESIS IN NATURE CONSERVATION ENGINEERING

TEMPORAL VARIATION IN ATMOSPHERIC POLLUTANT CONCENTRATIONS IN HUNGARY: A COMPARATIVE STUDY PRE, DURING AND POST PANDEMIC THROUGH THE USE OF DATA FROM THE SENTINEL-5P TROPOMI SATELLITE

Darwin Israel Muñoz Chamba

Sopron

2026

TASK STATEMENT

Title: Temporal variation in atmospheric pollutant concentrations in Hungary: a comparative study pre, during and post COVID-19 pandemic through the use of data from the SENTINEL-5P TROPOMI satellite

Name of student: Darwin Israel Muñoz Chamba, FOFAM2, nature conservation engineering MSc.

Supervisors: Dr. Pál Balázs assistant professor, University of Sopron, Faculty of Forestry, Institute of Environmental Protection and Nature Conservation

Detailed terms:

1. Prepare a literature review on main air pollutants, their sources, and their negative effects.
2. Introduce the background of assessing air quality by remote sensing.
3. Analyse the spatial-temporal variations of air pollutants and their relationship with the COVID-19 pandemic in Hungary.
4. Evaluate the results and their reliability.

The length of the thesis is not limited. Please prepare your thesis in accordance with the formal requirements for this type of work, submit one copy and upload it to the university repository in pdf format, identical to the example attached, by the deadline specified in the study timetable for the actual academic year.

Sopron, 18.02.2026

Prof. Dr. Tamás Rétfalvi
Professor, Head of Institute

Approve:

Prof. Dr. Bálint Heil
Professor, Dean

Dr. Gergely Zagyvai
Associate Professor, Coordinator

STATEMENT

I, Darwin Israel Muñoz Chamba. the undersigned, (Neptune Code: FOFAM2) signing this statement, declare that the titled: TEMPORAL VARIATION IN ATMOSPHERIC POLLUTANT CONCENTRATIONS IN HUNGARY: A COMPARATIVE STUDY PRE, DURING AND POST COVID-19 PANDEMIC THROUGH THE USE OF DATA FROM THE SENTINEL-5P TROPOMI SATELLITE

Thesis

is **my independent work**, during the preparation of the dissertation I abided *the rules of the copyright law LXXVI of 1999* and the regulations of the university concerning the preparation of the thesis, with regard to references and quotations.[9]

I also declare that during the preparation of the dissertation **I did not mislead** the consultant or the instructor who gave the on working independently.

By signing this statement, I acknowledge that if it can be proved that the thesis **was not written by myself** or there is a copyright infringement in relation to my thesis, the University of Sopron **refuses to accept the dissertation and institutes disciplinary proceedings against me.**

The refusal to accept the dissertation and the initiation of disciplinary proceedings shall not affect the additional legal consequences of the infringement (civil law, infringement law, criminal law).

17th April 2026 in Sopron

……
signature

1999 LXXVI law Article 34 § (1) Any part may be cited from a disclosed work by the source and naming the author indicated as such.
Such citation shall be true to the original and its scope shall be justified by the nature and purpose of the borrowing work.
Section 36 (1) details of publicly held lectures and other similar works, as well as political speeches for information purposes – to the extent justified by the purpose
– may be freely used. In the case of such use, the source, together with the author's name, must be indicated unless it proves to be impossible.

DARWIN ISRAEL MUÑOZ CHAMBA
2026
MSC in Nature Conservation Engineering
Soproni Egyetem
Erdőmérnöki Kar

Consultant: Dr. Balázs Pál PhD
adjunktus

A LÉGKÖRI SZENNYEZŐ ANYAGOK KONCENTRÁCIÓINAK IDŐBELI VÁLTOZÁSA MAGYARORSZÁGON: ÖSSZEHASONLÍTÓ VIZSGÁLAT A PANDÉMIA ELŐTT, ALATT ÉS UTÁN A SENTINEL-5P TROPOMI MŰHOLD ADATAINAK FELHASZNÁLÁSÁVAL

TEMPORAL VARIATION IN ATMOSPHERIC POLLUTANT CONCENTRATIONS IN HUNGARY: A COMPARATIVE STUDY PRE, DURING AND POST PANDEMIC THROUGH THE USE OF DATA FROM THE SENTINEL-5P TROPOMI SATELLITE

A légszennyezés az egyik legjelentősebb környezeti kihívás, amely hatással van az ökoszisztémákra, a növényzetre és az emberi egészségre, ezért kulcsfontosságú a természetvédelmi megoldások kidolgozásában. A légköri szennyező anyagok időbeli dinamikájának és az antropogén tevékenységekkel való kapcsolatának megértése elengedhetetlen a hatékony környezetgazdálkodáshoz. A COVID–19 világjárvány egyedülálló lehetőséget nyújtott annak vizsgálatára, hogy az emberi tevékenységek változásai hogyan befolyásolják a légszennyező anyagok koncentrációját regionális és városi léptékben.

A tanulmány a nitrogén-dioxid (NO_2), a szén-monoxid (CO) és a kén-dioxid (SO_2) koncentrációinak időbeli változását vizsgálja Magyarországon a Sentinel-5P TROPOMI műhold adatai alapján. Az elemzés a pandémia előtti, alatti és utáni időszakokat öleli fel, a szennyező anyagok viselkedésének és szezonális dinamikájának feltárása érdekében. Mindhárom szennyező anyag egyértelmű szezonális mintázatot mutatott, magasabb koncentrációkkal a hidegebb hónapokban. A NO_2 2020-ban jelentős csökkenést mutatott, majd 2021-ben újra növekedés következett. A CO összetettebb viselkedést mutatott, mivel országos szinten csökkent, ugyanakkor városi szinten magasabb értékek maradtak fenn. A SO_2 mutatta a legnagyobb változékonyságot és gyenge reakciót a korlátozásokra.

Összességében az eredmények azt mutatják, hogy a levegőminőség változásai szennyezőanyag-specifikusak és nagymértékben a kibocsátási forrásoktól függenek. Míg a NO_2 szorosan kapcsolódik a közlekedéshez, a CO és a SO_2 inkább állandó forrásokhoz, például a lakossági fűtéshez és az energiatermeléshez köthető. Az eredmények hangsúlyozzák a távérzékelés és a mérnöki megközelítések integrálásának fontosságát a légszennyezés dinamikájának jobb megértése érdekében.

DARWIN ISRAEL MUÑOZ CHAMBA
2026
MSC in Nature Conservation Engineering
University of Sopron
Faculty of Forestry

Consultant: Dr. Pál Balázs PhD
assistant professor

TEMPORAL VARIATION IN ATMOSPHERIC POLLUTANT CONCENTRATIONS IN HUNGARY: A COMPARATIVE STUDY PRE, DURING AND POST PANDEMIC THROUGH THE USE OF DATA FROM THE SENTINEL-5P TROPOMI SATELLITE

Air pollution is one of the most significant environmental challenges affecting ecosystems, plants and human health, making it a key area for finding solutions to conserve the natural elements involved. Understanding the temporal dynamics of atmospheric pollutants and their relationship with anthropogenic activities is essential for developing effective conservation strategies. COVID-19 pandemic offered a unique opportunity to study how changes in anthropogenic activities influence air pollutant concentration at regional and urban scales.

This study analyzes the temporal variation of nitrogen dioxide (NO_2), carbon monoxide (CO) and sulfur dioxide (SO_2) in Hungary, using data from the Sentinel-5P TROPOMI. The analysis covers pre-pandemic, pandemic and post-pandemic periods, for identifying changes in pollutant behavior and seasonal dynamics.

The results indicate that all three pollutants exhibit clear seasonal patterns, characterized by higher concentrations during colder months and lower levels during warmer periods. NO_2 showed the most pronounced decrease during 2020 and a rebound effect in 2021, with concentrations increasing and, in some cases, surpassing pre-pandemic levels. CO exhibited a more complex response. Although an apparent decrease during the pandemic period was observed at a country scale; relatively higher concentrations were observed on the city scale. SO_2 showed the highest variability and the weakest response to lockdown measures. Despite a slight reduction was observed, its behavior was characterized by fluctuations and peaks, specifically in early 2021.

Overall, the results demonstrate that air quality responses to COVID-19 restrictions are pollutant specific and largely determined by emission sources. While NO_2 is strongly linked to traffic and mobility, CO and SO_2 reflect more complex dynamics associated with stationary sources.

TABLE OF CONTENTS

1. INTRODUCTION 1

OBJECTIVES 3

GENERAL OBJECTIVE: 3

SPECIFIC OBJECTIVES: 3

2. LITERATURE REVIEW 4

2.1. Atmospheric Pollutants 4

2.2. Primary pollutants 4

2.3. Secondary pollutants 6

2.4. Sources of air pollution 7

2.5. Effects of pollutants on human health 9

2.6. Effects of pollutants on plants 10

2.7. Remote Sensing 11

2.7.1. Sentinel-5P TROPOMI Technology 11

2.7.2. Geographic Information Systems (GIS) 12

2.7.3. GIS Subsystems 13

2.7.4. Elements of GIS 13

2.7.5. Google Earth Engine (GEE) 14

3. METHODOLOGY 15

3.1. Study area 15

3.2. Data downloading 16

3.3. Temporal Period Definition 17

3.4. Data Processing 17

3.5. Temporal Segmentation 18

3.6. Spatiotemporal analysis of the concentration levels CO, NO_2 and SO_2 18

Seasonal Cycle and Annual Behavior Analysis 18

3.7. Geospatial and statistical analysis to compare the concentrations CO, NO_2 and SO_2. 20

4. RESULTS 22

4.1. Spatiotemporal analysis of the concentration levels of carbon monoxide (CO), nitrogen dioxide (NO_2), and sulfur dioxide (SO_2) during the years 2018–2023 using satellite images from the Sentinel-5P TROPOMI satellite. 22

5. DISCUSSION 40

5.1. Pollutant seasonal patterns and concentrations 40

5.2. Pollutants and temperature 42

6. CONCLUSIONS 43

7. BIBLIOGRAPHY 45

8. ATTACHMENTS I

1. INTRODUCTION

Air pollution is defined as any atmospheric condition in which certain substances are present at concentrations that can produce undesirable effects on human health and the environment. These substances include gases such as sulfur oxides (SOx), nitrogen oxides (NOx), carbon monoxide (CO), hydrocarbons, particulate matter such as smoke and aerosols, and other compounds suspended in the atmosphere (Admassu & Wubeshet, 2014).

Air pollutants are commonly found in higher concentrations in urban areas due to the strong presence of anthropogenic activities such as transportation, industrial production and energy generation. Air pollution is a modern challenge, not only for its role in climate change but also for its serious repercussions on both public and personal well-being, leading to higher instances of sickness and mortality (Gul & Das, 2023). Ambient air pollution is among the greatest environmental risks to human health, and it was responsible for 4.2 million deaths in 2016 worldwide (WHO, 2020)

Sulphur dioxide (SO_2) is an atmospheric pollutant primarily produced during combustion of sulfur-containing fossil fuels such as coal and oil. Exposure to SO_2 has been associated with several adverse health effects, particularly affecting the respiratory system. Short-term exposure can cause respiratory symptoms such as coughing, dyspnea, airway irritation and increased airway resistance, especially among individuals with asthma or other respiratory conditions. Long-term exposure has been linked to decreased lung function and increased prevalence of respiratory diseases. Sulfur dioxide is considered a respiratory tract irritant that can contribute to acute respiratory symptoms and may aggravate pre-existing cardiopulmonary diseases (Chen, Gokhale, Shofer, & Kuschner, 2007).

Nitrogen dioxide (NO_2) is an atmospheric pollutant, which its primary source is the combustion of fossil fuels and motor vehicle use (Atkinson et al., 2018). Contributes to the creation of smog and acid rain (Chen et al., 2007). Studies have shown that this pollutant is related to respiratory, cardiovascular diseases and premature mortality (Huang et al., 2021), nevertheless, some studies have reported discrepancies as to whether or not this pollutant directly affects health in certain populations (Bentayeb et al., 2015). These discrepancies may be related to differences in geographic location, study design, exposure assessment, and population characteristics (Liu et al., 2019).

Carbon monoxide (CO) is a colorless, odorless and tasteless toxic gas, produced by the incomplete combustion of carbonaceous fuels such as wood, petrol, coal, natural gas and kerosene (WHO, 2010). Anthropogenic emissions are responsible for about two thirds of the carbon monoxide in the atmosphere and natural emissions account for the remaining one third.

CO exposure is linked to hypoxia and high levels exposures can cause unconsciousness and death. Evidence is also mounting that carbon monoxide can produce a cascade of cellular events leading to adverse effects that are not necessarily ascribable to hypoxia (WHO, 2010).

During the pandemic in 2020, the world was forced to stop its activities during the lockdown. Mobility restrictions were the strongest measures taken by governments to prevent massive spread of the virus, and although it was not intended, it may have had an impact on the concentration of the pollutants in the atmosphere.

In Hungary, restrictions associated with the COVID-19 pandemic began in March 2020. These restrictions reduced vehicular traffic and several economic activities, creating conditions that potentially influenced atmospheric pollutant concentrations.

This study analyzes the temporal variation of carbon monoxide (CO), nitrogen dioxide (NO_2), and sulfur dioxide (SO_2) in Hungary between 2018 and 2023 using satellite data from the Sentinel-5P TROPOMI sensor. The study combines geospatial analysis and statistical evaluation to identify temporal patterns and compare pollutant concentrations during the pre-pandemic, pandemic and post-pandemic periods.

From a conservation perspective, understanding air pollution dynamics is essential for protecting ecosystem integrity and maintaining the balance between natural and anthropogenic systems. Air pollution not only has a deep effect on human health but also has a significant impact on vegetation, soil processes, and biodiversity, influencing ecosystem health and interactions too. That is why it is so important to analyze the temporal behaviors of pollutants in order to contribute to the development of more effective environmental management strategies, supporting sustainable land use, climate adaptation, and conservation planning.

OBJECTIVES

GENERAL OBJECTIVE:

Determine concentration levels of CO, NO_2, SO_2 present in the air of Hungary by using satellite data from the Sentinel-5P TROPOMI Satellite.

SPECIFIC OBJECTIVES:

- Conduct a spatiotemporal analysis of the concentration levels of carbon monoxide (CO), nitrogen dioxide (NO_2), sulfur dioxide (SO_2) during the years 2018-2023 using satellite images from the Sentinel-5P TROPOMI satellite.
- Use a geospatial and statistical analysis to compare the concentrations of carbon monoxide (CO), nitrogen dioxide (NO_2), sulfur dioxide (SO_2) during the pre-pandemic, during, and post-pandemic periods in major cities in Hungary

2. LITERATURE REVIEW

2.1.Atmospheric Pollutants

The atmosphere can be defined as the relatively thin gaseous envelope that surrounds the entire planet Earth. It possesses several properties related to its physical state and chemical composition, and it undergoes a variety of internal processes and external interactions that can maintain or alter these properties (Singh, 1995). The atmosphere is composed of 78% nitrogen (N), 21% oxygen (O), and the remaining 1% consists of hydrogen (H), argon (Ar), neon (Ne), helium (He), and carbon dioxide (CO_2) (Ackerman y Knox, 2007).

Air pollution can be defined as a mixture of hazardous substances of both natural and anthropogenic origin that are released into the atmosphere. Some of these hazardous substances are emitted naturally, such as ash and gases from volcanic eruptions. Other emissions may result from both human and natural activities, such as smoke from forest fires, as well as methane, which originates from the decomposition of organic matter in soils and in animal feeding operations (Rice et al., 2021).

Pollution is caused by solids, liquids, and certain gases that remain suspended in the air. The main sources of air pollution generated by human activities include vehicle exhaust emissions, manufacturing plants, dust, volcanoes, and fires. Solid and liquid particles suspended in the air are referred to as aerosols (Sarla, 2020).

The standard classification of pollutants can be divided into two types:

2.2. Primary pollutants

These are those that are emitted directly from a source. Examples include nitrogen oxides (NOx), sulfur oxides (SOx), volatile organic compounds (VOCs), particulate matter (PM), and carbon oxides (CO_2 + CO).

The main primary pollutants are:

Nitrogen Dioxide (NO_2)

This group includes nitric oxide (NO), nitrogen dioxide (NO_2), nitrous oxide (N_2O), dinitrogen trioxide (N_2O_3), and dinitrogen pentoxide (N_2O_5). These oxides are produced by natural phenomena such as lightning, volcanic eruptions, and bacterial activity in soils, as well as by anthropogenic sources such as fuels used in internal combustion engines, thermal

power plants, industrial facilities, heating systems, and incinerators. NO and NO_2, collectively referred to as NOx, are the main nitrogen oxides emitted by vehicles (Onursal y Gautam, 1984).

Sulfur Dioxide (SO_2)

Sulfur dioxide (SO_2) is a stable, non-flammable, non-explosive, and colorless gas that is highly soluble in water. It is primarily produced by the combustion of sulfur-containing fossil fuels during thermal power generation, heating, cooking, and transportation. In the atmosphere, SO_2 can be oxidized to sulfur trioxide (SO_3) through reactions with oxygen. Global SO_2 emissions are estimated to reach 294 million tons annually, of which approximately 160 million tons are of anthropogenic origin (Onursal & Gautam, 1984).

SO_2 is produced from both natural and anthropogenic sources. Volcanic activity represents the main natural source, whereas the combustion of fossil fuels containing sulfur, such as oil and coal, constitutes the primary anthropogenic source (Khalaf et al., 2024). Activities such as thermal power generation—particularly in coal-fired power plants—metal smelting, oil extraction, fuel consumption, and transportation significantly contribute to SO_2 emissions (Khalaf et al., 2024).

In the atmosphere, SO_2 can dissolve in water vapor to form acidic compounds and can interact with other gases and particles to produce sulfates and other respirable particulate matter (Chen et al., 2007).

Carbon Monoxide (CO)

It is a colorless, odorless gas that is slightly denser than air and is emitted from both natural and anthropogenic sources. Anthropogenic sources generate CO through the incomplete combustion of carbon-based fuels in motor vehicles, heating systems, industrial facilities, thermal power plants, and incinerators. Among these, motor vehicles are the largest contributors to CO emissions. The conversion of CO to CO_2 in the atmosphere takes between two and five months (Onursal y Gautam, 1984).

Emissions from spark-ignition engines are released through exhaust, crankcase, and fuel system. The main pollutants emitted by gasoline-powered vehicles include CO, hydrocarbons (HC), NOx, and lead (Onursal & Gautam, 1984).

Methane (CH_4)

Methane is one of the main greenhouse gases. Its primary emission sources include anaerobic decomposition in natural wetlands, flooded rice fields, livestock production systems, biomass burning, anaerobic decomposition of organic waste in landfills, and the release of fossil methane during the exploration and transportation of fossil fuels.

It is evident that anthropogenic activities play a significant role in increasing methane emissions in most of these sources, particularly through the expansion of rice cultivation, livestock production, and the exploration and use of fossil fuels (Heilig, 1994).

Particulate Matter (PM)

Particulate matter consists of fine solid particles and liquid droplets, excluding pure water, that are dispersed in the air. These originate from both natural and anthropogenic sources. Natural sources include windblown dust, volcanic ash, forest fires, sea salt, and pollen. Anthropogenic sources include thermal power plants, industrial activities, commercial and residential facilities, and motor vehicles that use fossil fuels (Onursal y Gautam, 1984).

Particles with an aerodynamic diameter of 10 μm or less are known as inhalable suspended particles or PM10, these particles remain in the atmosphere for longer periods due to their low settling velocities and can penetrate deeply into the respiratory tract. The main sources of PM10, or coarse particles, include windblown dust, vehicles traveling on unpaved roads, material handling, and crushing and grinding operations (Onursal y Gautam, 1984).

2.3. Secondary pollutants

Formed through chemical reactions between different primary pollutants or with natural constituents in the atmosphere. Examples include ozone (O_3) and peroxyacyl nitrates (PAN).

Ozone (O_3)

Ozone is a colorless gas found in two distinct layers of the atmosphere. In the stratosphere, ozone is formed through the photolysis of oxygen or naturally occurring hydrocarbons and plays a crucial role in protecting the Earth from ultraviolet radiation. In the troposphere, ground-level ozone is formed because of reactions between volatile organic compounds (VOCs) and NOx in the presence of sunlight and high temperatures. Ground-level ozone is one of the main components of smog in urban areas, and motor vehicles are the primary anthropogenic source of its precursors (Onursal y Gautam, 1984).

2.4. Sources of air pollution

Natural sources of pollution

Naturally occurring particulate matter (PM) includes dust from the Earth's surface (crustal material), sea salt in coastal areas, and biological material such as pollen, spores, or plant and animal debris (Delon, 2018). Volcanic eruptions can introduce significant amounts of gases and particles into the atmosphere (Pénard-Morand & Annesi-Maesano, 2004).

Other natural sources of air pollution include lightning, which produces significant amounts of nitrogen oxides (NOx); algae on ocean surfaces that emit hydrogen sulfide (H_2S); wind erosion, which introduces particles into the atmosphere; and wetlands such as swamps, peatlands, or shallow lakes, which produce methane (CH_4). Low concentrations of O_3 also occur naturally at ground level, formed in the presence of sunlight through reactions between NOx and volatile organic compounds (VOCs) (Pénard-Morand y Annesi-Maesano, 2004).

Anthropogenic sources

In urban areas, most air pollution originates from human-made sources. These sources can be classified as mobile (cars, trucks, aircraft, marine engines, etc.) or stationery (factories, power plants, etc.) (*Figure 1*) (Pénard-Morand y Annesi-Maesano, 2004).

Vehicular traffic represents the main source of air pollution in large cities of industrialized countries. The combustion of carbon-based fuels (coal, gasoline, wood, natural gas) is never complete and produces carbon monoxide (CO) and hydrocarbons. Nitrogen oxides (NOx) are generated from the combination of nitrogen in the air and oxygen during the high-temperature combustion of fossil fuels in engine systems (Pénard-Morand y Annesi-Maesano, 2004).

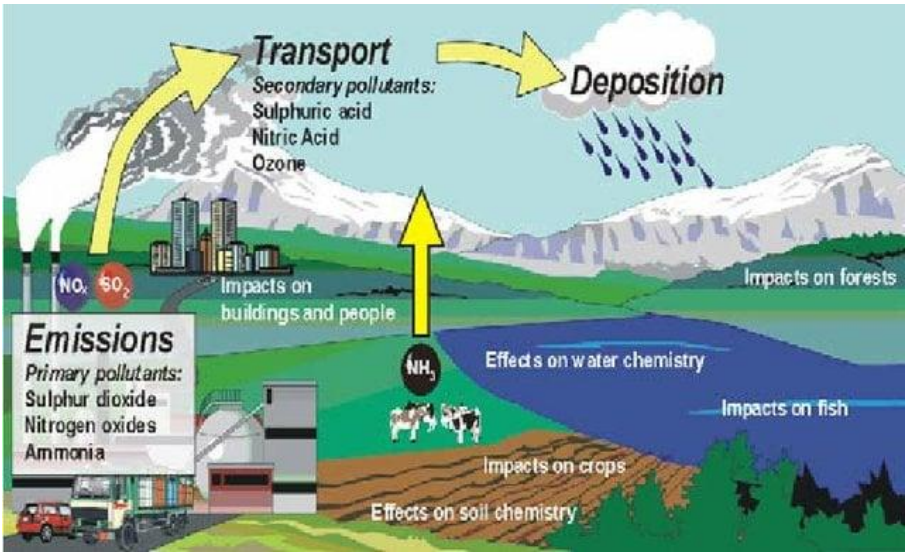

Figure 1: Air pollution pathway
Source: Haq & Schwela (2008) p. 11.

Human activities have increased the concentration of volatile organic compounds (VOCs) due to the huge amount of petroleum use, chemical industries, and transportation, while nitrogen oxides (NOx) mainly originate from combustion processes in power plants and automobiles. As a result, ozone (O_3) concentrations increase, leading to higher levels of smog in densely populated and industrialized regions. Human activities also contribute significantly to total ambient particulate matter (PM). In urban environments, particles are primarily generated as a result of the combustion of both mobile and stationary sources. Coal and sulfur present in fuel oils are oxidized into sulfur dioxide (SO_2). These fuels are widely used for transportation, heating, and providing the energy required for numerous industrial processes. Additionally, industrial activities generate specific pollutants as by-products, such as fluorine- or aluminum-derived compounds (Pénard-Morand y Annesi-Maesano, 2004).

Mineral processing releases heavy metals such as cadmium, zinc, and lead. Mercury is produced through the incineration of domestic waste. Agricultural activities, particularly through the use of nitrogen-based fertilizers, generate nitrous oxide (N_2O), a greenhouse gas, and ammonia (NH_3), both of which contribute to acidification processes. Methane (CH_4), another greenhouse gas, is mainly produced through the digestion and excretion processes of livestock (Pénard-Morand y Annesi-Maesano, 2004).

2.5. Effects of pollutants on human health

Nitrogen Dioxide (NO_2).

It is a reactive gas that can cause bronchitis and pneumonia, while also increasing susceptibility to respiratory infections. It affects both the cellular and humoral immune systems, impairing immune responses. According to Hasselbald et al. (1992) children are more prone to respiratory diseases due to exposure to NO_2, and another study conducted by Saldiva et al. (1994) has associated NO_2 exposure with increased daily mortality in children under five years of age. Individuals exposed to NO_2 are at risk of developing chronic bronchitis, particularly those with pre-existing chronic respiratory diseases and emphysema.

Sulfur Dioxide (SO_2).

Numerous single- and multi-pollutant time-series studies have demonstrated associations between SO_2 exposure and daily mortality and morbidity. SO_2 is also linked to allergic reactions such as rhinitis, with symptoms including nasal congestion and sneezing; long-term exposure may lead to more severe conditions such as atopy. High levels of SO_2 inhalation have been associated with increased release of white blood cells and their precursors from the bone marrow, as well as elevated counts of band cells in peripheral blood. Additionally, SO_2 exposure can cause damage to developing fetuses and to the reproductive system, particularly the testes, potentially leading to increased morbidity and mortality, as well as low birth weight. At the molecular level, SO_2 reduces immune function, increases membrane permeability, induces chromosomal breakage, and exhibits mutagenic properties (Sonwani y Saxena, 2021).

High doses of inhaled SO_2 have also been associated with acute neurotoxic effects, including peripheral neuritis, seizures, agitation, tremors, vertigo, and fever. Liquid SO_2, under conditions of high pressure or low temperature, can cause severe corneal damage. The cornea may turn gray, followed by swelling of the eyelids after a few hours. As a result, the conjunctiva may become white and opaque, and thrombosis in ocular blood vessels may occur. Direct skin contact with SO_2 can also lead to dermatological reactions such as urticaria. At high doses, SO_2 causes severe skin irritation, resulting in pain, redness, and blistering. Furthermore, SO_2 has been shown to inhibit DNA synthesis and cause chromosomal damage, as observed in workers in sulfuric acid production facilities (Sonwani y Saxena, 2021).

Carbon Monoxide (CO).

CO has been strongly associated with cardiovascular diseases and Parkinsons disease. The affinity of hemoglobin for CO is much higher than oxygen, which can bring adverse health effects by reducing delivery of oxygen (Blomberg et al., 1999). CO enters the bloodstream through the lungs and attaches to hemoglobin (Hb), forming caboxyhemoglobin (COHb) and thereby reducing the amount of oxygen (O_2) delivered to the body's organs and tissues. High COHb concentrations are poisonous. Central nervous system effects in individuals suffering from acute CO poisoning cover a wide range, depending on severity of exposure: headache, dizziness, weakness, nausea, vomiting, disorientation, confusion, collapse and coma (Raub & Benignus, 2002)

2.6. Effects of pollutants on plants

Air pollution can also cause significant damage to plants. It affects plant health by altering their physiology, biochemistry, and morphology. Different atmospheric gases lead to a variety of visible symptoms, resulting in reduced plant growth and productivity.

Physiological and biochemical responses in plants can serve as indicators of environmental conditions. In air pollution studies, biomonitoring has become an important concept. Certain plant species act as indicators when exposed to air pollutants, producing a range of symptoms, particularly morphological ones that vary depending on the type of pollutant. Therefore, plants can serve as valuable tools in methods for monitoring and controlling air pollution. These types of plants are generally classified as "sensitive" species. For biomonitoring purposes, the Air Pollution Tolerance Index (APTI) is used to classify plants into categories such as tolerant, moderately tolerant, sensitive, and highly sensitive. Tolerant species act as "sinks" for pollutants, while sensitive species function as "indicators" (Shannigrahi, Fukushuma & Sharma, 2004).

Plants interact with air pollutants by adsorbing, accumulating, or absorbing them into their tissues. If the pollutant is toxic, it can cause injury and produce symptoms, particularly morphological damage. Tolerant plant species contribute to pollutant removal, thereby helping to reduce the overall pollution load. Air pollutants can also damage leaf cuticles and affect stomatal conductance. In addition, they can interfere with photosynthetic systems, respiration rates, and carbon allocation patterns within plants. The impact of air pollutants on plant health can be classified into two main types: direct effects, through visible injuries

such as chlorosis and necrosis, and indirect effects, through alterations in growth and reproduction processes (Weinstein, 1977).

2.7. Remote Sensing

Remote sensing is the science and art of obtaining information about an object, area, or phenomenon through the analysis of data acquired by a device that is not in direct contact with the object, area, or phenomenon under study. In many respects, remote sensing can be understood as a process of interpretation or "reading." By using different sensors, data is collected remotely and later analyzed to extract information about objects of interest. The information acquired remotely can take different forms, including variations in force distribution, acoustic wave propagation, or electromagnetic energy distribution (Lillesand, Kiefer, y Chipman, 2015).

Satellite imagery is the result of using remote sensors mounted on satellites, which capture images of the Earth's surface under specific characteristics that depend on both the satellite platform and the sensor employed (Alvarez, 2014).

Satellite sensors receive information about an object through electromagnetic energy. This information may be encoded in the frequency, intensity, or polarization of the wave and can be transmitted either directly from the object or indirectly through reflection, scattering, or re-emission before reaching the sensor. All materials on Earth reflect or emit electromagnetic energy. Sensors measure the intensity of this radiation and analyze its variation across different frequencies to determine the physical properties of the observed objects (García, 2000).

2.7.1. Sentinel-5P TROPOMI Technology

The Tropospheric Monitoring Instrument (TROPOMI) is on board the Sentinel-5 Precursor satellite. It represents the first Copernicus mission developed by the European Space Agency (ESA) specifically designed for atmospheric monitoring. The sensor is a nadir-viewing imaging spectrometer that operates across multiple spectral ranges, including ultraviolet-visible (270–500 nm), near-infrared (710–770 nm), and shortwave infrared (2314–2382 nm) (Eskes et al., 2021).

The instrument uses passive remote sensing techniques to achieve its objectives by measuring solar radiation that is reflected and emitted by the Earth at the top of the atmosphere. It captures images of a swath of the Earth on a two-dimensional detector over

approximately one second, during which the satellite travels about 7 km. This swath has approximate dimensions of 2600 km in the direction perpendicular to the satellite's path and 7 km along the track. After each one-second measurement, a new measurement begins, allowing the instrument to continuously scan the Earth as the satellite moves (Eskes et al., 2021).

The two dimensions of the detector are used to capture different ground pixels across the swath and to resolve different wavelengths. The measurement principle of TROPOMI is illustrated in (*Figure 2*) (Eskes et al., 2021).

The sensor acquires data with an approximate spatial resolution of 1 km and a daily temporal resolution. TROPOMI provides information on atmospheric concentrations of O_3, NO_2, SO_2, CO, CH_4, CH_2O, and aerosols, representing a significant advantage compared to other satellite systems (Veefkind et al., 2012).

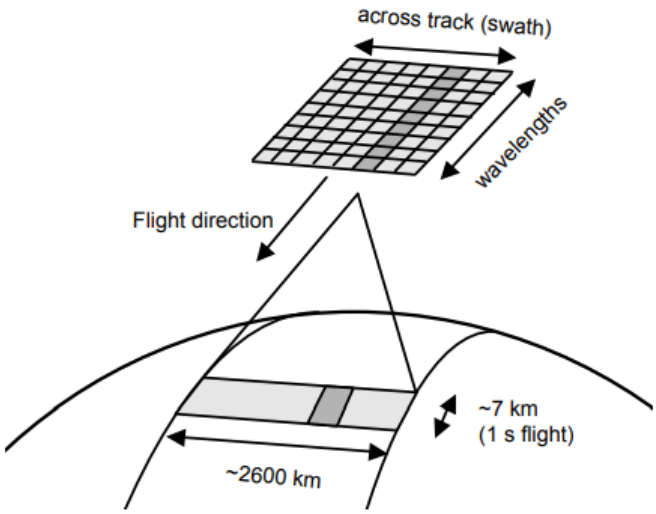

Figure 2: TROPOMI measuring principle
Source: Eskes et al. (2021).

2.7.2. Geographic Information Systems (GIS)

Geographic Information Systems (GIS) are computer-based systems capable of handling virtually any type of information related to features that can be referenced by their geographic location. These systems can manage both spatial (location-based) data and attribute data associated with those features. In other words, GIS not only enables automated

mapping and visualization of feature locations but also provides the capability to store and analyze descriptive characteristics ("attributes") of those features (Lillesand et al., 2015).

GIS allows the following operations to be performed:

- Reading, editing, storing, and managing spatial data.
- Analysis of such data. This can range from simple queries to the development of complex models and can be carried out on both the spatial component of the data (the location of each value or element) and the thematic component (the value or the element itself).
- Generation of outputs such as maps, reports, graphs, and other visual products (Olaya, 2014).

2.7.3. GIS Subsystems

According to Olaya (2014), to fully understand GIS, it should be considered as a set of subsystems, each responsible for specific functions. These are:

Data subsystem: Responsible for data input and output operations, as well as data management within the GIS. It allows other subsystems to access and operate based on this data.

Visualization and cartographic production subsystem: Responsible for generating representations from data (maps, legends, etc.), enabling interaction with the information.

Analysis subsystem: Contains the methods and processes used for analyzing geographic data.

According to Olaya (2014), for a GIS to be considered a useful and comprehensive tool, it must incorporate these three subsystems to some extent.

2.7.4. Elements of GIS

Traditionally, five main elements are considered fundamental in GIS (*Figure 3*):

Data: The raw material required for GIS analysis.

Methods: A set of procedures and methodologies applied to the data.

Software: Specialized programs used to process data and implement analytical methods.

Hardware: The equipment required to run the software.

People: The individuals responsible for designing, operating, and utilizing the system (Olaya, 2014).

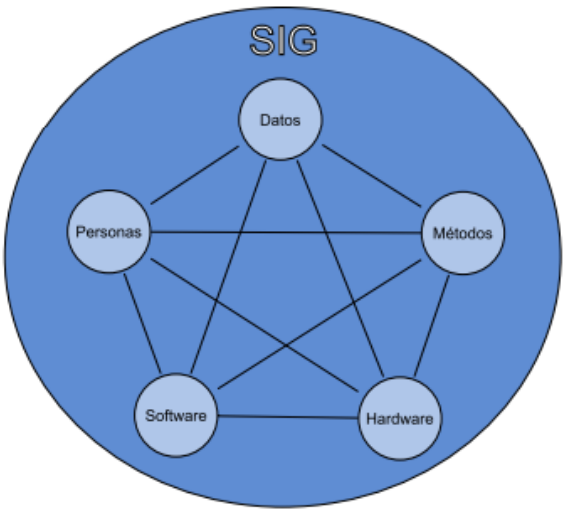

Figure 3: GIS elements
Source: Olaya (2014) p.15

2.7.5. Google Earth Engine (GEE)

Google Earth Engine (GEE) is a platform developed by Google that enables large-scale geospatial processing. One of its main objectives is to reduce the time required for data processing and to facilitate analyses based on spatial information. GEE emerged from the need to efficiently manage the large volumes of data generated by space missions dedicated to collecting remote sensing information. To achieve this, Google developed an infrastructure based on three key components: a data catalog, computational capacity, and application programming interfaces (APIs). GEE compiles geospatial information from multiple sources around the world and stores copies of these datasets within its own data centers, enabling the storage of more than 20 petabytes (20,000,000 gigabytes) of information in a single platform (Solórzano Villegas & Perilla Suárez, 2022).

3. METHODOLOGY

3.1. Study area

The analysis was initially conducted across the entire territory of Hungary (*Figure 4*), where average concentration values of each pollutant were calculated. Subsequently, a more detailed analysis was carried out focusing on the cities with highest population density: Budapest, Szeged and Debrecen.

Hungary is a landlocked country located in the Carpatian (Pannonian or Central Danubian) Basin, in the southeastern part of Central Europe. It lies between 16°05′ and 22°58′ E longitude, and 45°48′ and 48°35′ N latitude, positioning it almost equidistant between the Equator and the North Pole. The country extends approximately 528 km from west to east and 268 km from north to south. Due to its central geographical location, Hungary is influenced by oceanic, continental, and Mediterranean air masses, making it a transitional climatic zone. Additionally, it is predominantly a lowland country, with around 83% of its territory situated below 200 meters above sea level, which has important implications for atmospheric circulation and pollutant dispersion processes (Hungarian Geographical Institute, 2012).

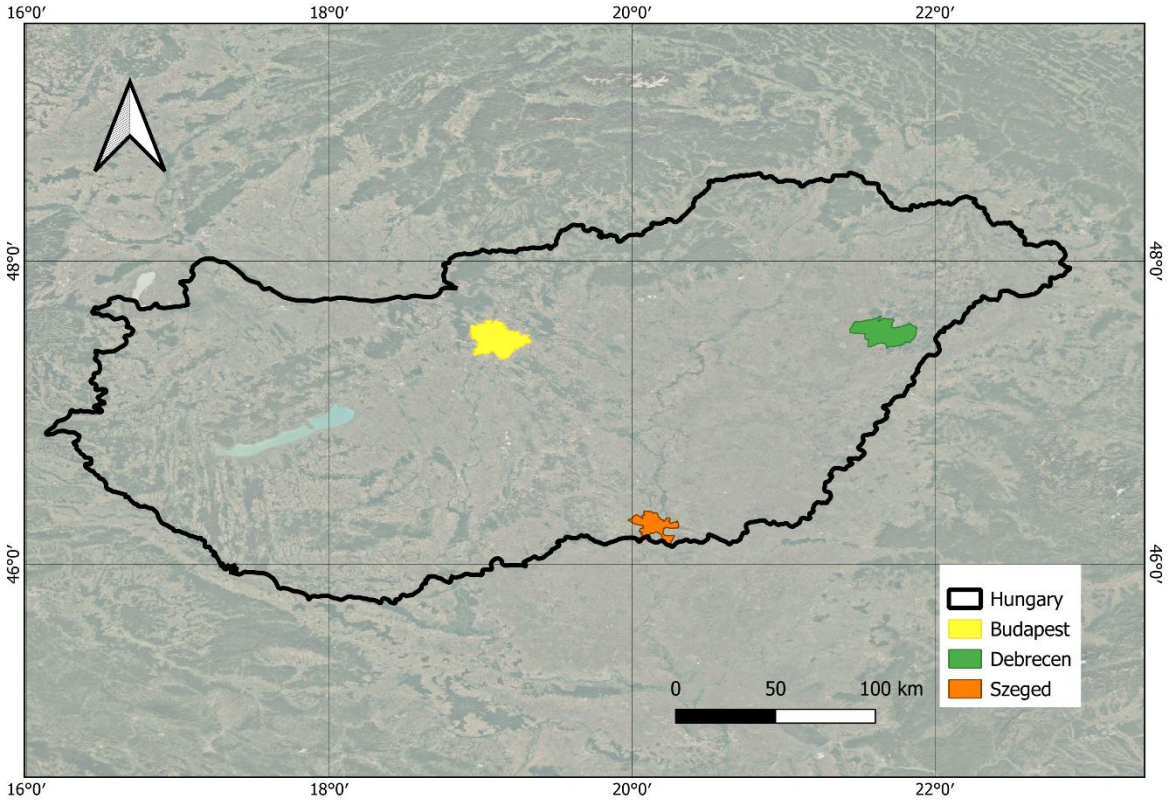

Figure 4. Hungary geographical localization
(Source: Own elaboration)

3.2. Data downloading

Atmospheric pollutant data were obtained from the Sentinel-5P satellite, equipped with the Tropospheric Monitoring Instrument (TROPOMI). The downloaded pollutants data included carbon monoxide (CO), nitrogen dioxide (NO_2) and sulfur dioxide (SO_2).

The datasets used correspond to the level 2 offline (OFFL) products available in the Google Earth Engine (GEE) catalog, including COPERNICUS/S5P/OFFL/CO, COPERNICUS/S5P/OFFL/NO_2, and COPERNICUS/S5P/OFFL/SO_2, with their corresponding bands (*Table 1*). These products provide column densities of atmospheric pollutants expressed in mol/m².

Data was accessed and processed using Goggle Earth Engine (GEE) platform. Specific scripts written in JavaScript were created within the GEE Code Editor to extract pollutant concentration data. The analysis was spatially constrained to the study area using administrative boundaries for Hungary and further refined for the selected urban areas: Budapest, Szeged and Debrecen.

Table 1. TROPOMI Sentinel-5P Satellite characteristics

Pollutant	Sensor/Band	Spatial resolution	Temporal Resolution	Unity
CO	CO_column_number_density	1x1 km	30 min	$mol/\ m2$
SO_2	SO_2_column_number_density_15km	1x1 km	30 min	$mol/\ m2$
NO_2	tropospheric_NO_2_column _number_density	1x1 km	30 min	$mol/\ m2$

Source: Earth Engine Data Catalog (2008)

3.3. Temporal Period Definition

Three temporal periods were defined to evaluate the impact of COVID-19 related mobility restrictions on air quality:

- **Pre-pandemic period:** January 2018 – February 2020
- **Pandemic period:** March 2020 – May 2020
- **Post-pandemic period:** June 2020 – December

These periods were established based on the onset of mobility restrictions and lockdown measures implemented across Europe in response to the COVID-19 pandemic.

3.4. Data Processing

The processing of satellite-derived atmospheric data was carried out using the Google Earth Engine (GEE) platform, which enables efficient handling of large geospatial datasets, initially spatial filtering was applied to constrain the analysis to the study area using administrative boundaries for Hungary, as well as polygon geometries representing the selected urban areas: Budapest, Szeged and Debrecen. This ensures that all values correspond to the defined regions of interest.

To improve data reliability, quality filtering procedures were implemented using the quality assurance (QA) bands provided in each dataset. Pixels with low-quality values, often associated with cloud cover, atmospheric or sensor limitations were excluded from the analysis.

Following the filtering process, daily observations were aggregated into monthly composites using statistical reducers, specifically the mean function.

For each pollutant and each spatial unit, a time series was generated covering the period from 2018 to 2023. These time series were structured to include both temporal (year and

month) and spatial (city or national level) attributes, facilitating subsequent statistical analysis.

The processed data were then exported from GEE as comma-separated values (.csv) files. Each dataset contained monthly average pollutant concentrations expressed in column number density (mol/m²), along with the corresponding timestamps and geographic identifiers.

Post-processing and further analysis were conducted in Python. Data cleaning procedures including handling missing values, verifying temporal continuity and standardizing data formats.

Overall, this processing workflow ensured high data quality, temporal consistency, and reproducibility, enabling a robust analysis of spatiotemporal patterns in atmospheric pollutant concentrations.

3.5. Temporal Segmentation

To evaluate the impact of COVID-19 related restrictions, the study period was defined into three phases:

- Pre-pandemic: January 2018 – February 2020

- Pandemic: March 2020 – May 2020

- Postpandemic: June 2020 – December 2023

This classification enables a structured comparison of pollutant concentrations under different levels of anthropogenic influence.

3.6. Spatiotemporal analysis of the concentration levels CO, NO_2 and SO_2

Seasonal Cycle and Annual Behavior Analysis

To study the temporal behavior of each pollutant, a seasonal analysis was performed based on the calculation of mean monthly concentrations across the entire study period.

For this, the dataset was grouped by month and the average concentration for each pollutant and each month was calculated. This approach allows the identification of the typical annual cycle by removing interannual variability and highlighting recurring seasonal patterns.

The resulting monthly averages were used to construct representative seasonal curves for CO, NO_2 and SO_2. These curves provide a simplified but robust representation of how pollutant concentrations vary throughout the year under typical conditions.

The analysis focused on identifying:

- Periods of maximum and minimum concentration.

- Recurring seasonal peaks.

- Differences in temporal behavior among pollutants.

- Consistency of patterns across the study period.

In addition to this, a comparative analysis was performed between the long-term seasonal cycle the actual behavior observed during the 2018-2023 period. For this purpose, time series plots were generated showing the monthly evolution of pollutant concentrations alongside the corresponding monthly mean values derived from the full dataset.

This comparison allows for the identification of deviations from the expected seasonal pattern, highlighting periods where pollutant concentrations differ from the typical annual behavior. Such deviations are particularly useful for detecting the influence of external factors, including changes in anthropogenic activity or anomalous environmental conditions.

Spatial Analysis and Mapping

To complete the analysis a spatial evaluation of pollutant distribution was conducted through the generation of mean concentration maps. These maps were created by calculating the average concentration of each pollutant over the study period and visualizing their spatial distribution across the country.

The spatial representation of pollutant concentrations allows for the identification of geographic patterns, highlighting areas with relatively higher or lower levels of atmospheric pollution.

3.7. Geospatial and statistical analysis to compare the concentrations CO, NO_2 and SO_2.

The second objective of this study consisted of performing a geospatial and statistical comparison of atmospheric pollutant concentrations (CO, NO_2, and SO_2) across different temporal periods associated with the COVID-19 pandemic in major Hungarian cities.

Comparative Analysis of Pollutant Concentrations Across COVID-19 Periods

The analysis was conducted using a dataset containing monthly average concentrations of CO, NO_2, and SO_2 for the cities of Budapest, Szeged, and Debrecen. These cities were selected due to their high population density and representativeness of urban environmental conditions in Hungary.

Each observation in the dataset included the following attributes: city, pollutant type, concentration value, and corresponding temporal period. Pollutant concentrations were expressed in column number density (mol/m^2), ensuring consistency with the satellite-derived data used throughout the study.

To facilitate comparison, the dataset was categorized into three distinct temporal periods:

- Pre-pandemic
- Pandemic
- Post-pandemic

These categories were defined according to the timeline of COVID-19 mobility restrictions in Europe.

Monthly data were grouped according to the defined temporal periods (pre-pandemic, pandemic, and post-pandemic), and average concentration values were calculated for each pollutant and city.

This aggregation allowed the transformation of the time series into a comparative framework, enabling a direct evaluation of how pollutant levels changed under different levels of anthropogenic activity. A spatial comparison was subsequently performed by analyzing differences in pollutant concentrations among the selected cities (Budapest, Szeged, and Debrecen), allowing the identification of location-specific patterns associated with factors such as traffic intensity, industrial activity, and energy consumption. This approach captures the heterogeneity of pollutant behavior at the urban scale, providing

insights that are not observable at the national level. To quantify temporal changes, percentage variations in pollutant concentrations were calculated for each city and pollutant between the defined periods. Specifically, the variation between the pandemic and pre-pandemic periods was computed as:

$$\Delta_{\text{pandemic}}(\%) = \frac{C_{\text{pandemic}} - C_{\text{pre}}}{C_{\text{pre}}} \times 100$$

and the variation between the post-pandemic and pandemic periods as:

$$\Delta_{\text{post}}(\%) = \frac{C_{\text{post}} - C_{\text{pandemic}}}{C_{\text{pandemic}}} \times 100$$

Where C represents the average pollutant concentration for the corresponding period. These metrics provide a clear and standardized measure of the magnitude and direction of change, allowing for consistent comparison across pollutants with different concentration ranges.

Correlation Analysis Between Pollutant Concentrations and Temperature

Monthly average temperature data for the selected cities (Budapest, Szeged, and Debrecen) were obtained from the Hungarian Meteorological Service (OMSZ) database (https://odp.met.hu), which provides historical climate observations. These data were temporally aligned with the pollutant concentration dataset to ensure consistency in the analysis period (2018–2023).

The temperature dataset was integrated with the pollutant time series based on matching temporal attributes (year and month), allowing for a direct comparison between atmospheric conditions and pollutant concentrations. Prior to analysis, the data were reviewed to ensure completeness and consistency, and any missing or inconsistent values were handled to maintain the integrity of the dataset.

To evaluate the relationship between air temperature and pollutant concentrations, a correlation analysis was performed using the Pearson correlation coefficient (r). This statistical measure quantifies the strength and direction of the linear relationship between two continuous variables. The coefficient was calculated for each pollutant and city

independently, allowing for the identification of pollutant-specific responses to temperature variability.

The Pearson correlation coefficient was computed as:

$$r = \frac{\sum_{i=1}^{n}(X_i - \bar{X})(Y_i - \bar{Y})}{\sqrt{\sum_{i=1}^{n}(X_i - \bar{X})^2}\sqrt{\sum_{i=1}^{n}(Y_i - \bar{Y})^2}}$$

Where X_i represents the pollutant concentration, Y_i the corresponding temperature value, and $\bar{X}$ and $\bar{Y}$ are the mean values of each variable.

This analysis allows the identification of inverse or direct relationships between temperature and pollutant concentrations. Negative correlation values indicate that pollutant concentrations tend to decrease as temperature increases, while positive values indicate the opposite behavior. The magnitude of the coefficient reflects the strength of the relationship, enabling the differentiation between weak, moderate, and strong correlations.

4. RESULTS

4.1. Spatiotemporal analysis of the concentration levels of carbon monoxide (CO), nitrogen dioxide (NO_2), and sulfur dioxide (SO_2) during the years 2018–2023 using satellite images from the Sentinel-5P TROPOMI satellite.

Pollutants behave in different ways throughout the months; this is clearly related to the seasonal changes. Although the three pollutants have their specific pattern, we can see that all of them tend to increase concentration around October-March and decreasing in April-September.

For NO_2, the peak concentration is in December-January, and then it drastically lowers in February-March, to reach the second peak of the year in April. For CO, the peak concentration is in March-April, to then drop in May-November, and then the concentration starts to rise till its peak in March again, both can be related to the start of agricultural activities. For SO_2, the peak concentration is in December-February. Then we can see it slowly drops in March-June caused by the rise in temperature. A secondary peak in summer (July) may be linked to agricultural activities as well as increased use of cooling systems and mobility during holiday seasons (*Figure 5*).

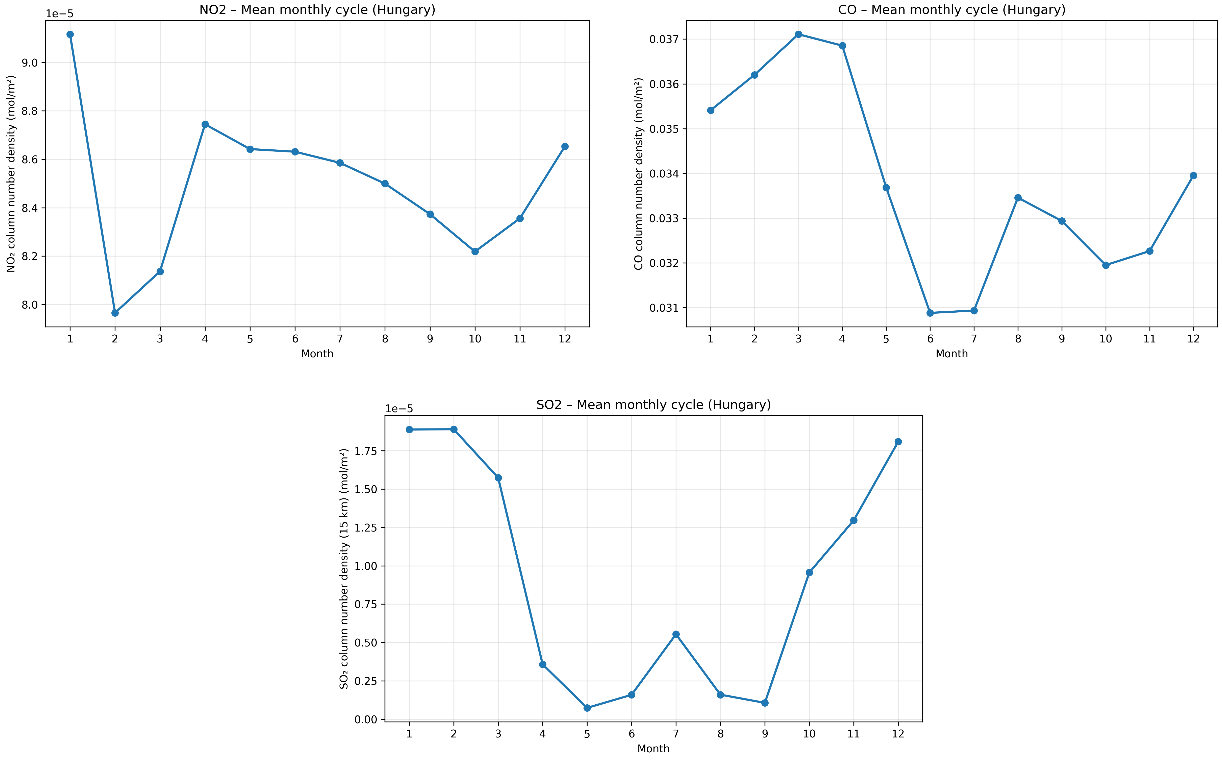

Figure 5: Pollutants monthly cycle.
Source: Own elaboration

As seen in *Figure 6*, the peak concentration for SO_2 was observed in February 2021, while the lowest concentration occurred in May 2019. Considering that COVID-19 restrictions in Hungary began on March 11, 2020, a noticeable reduction in SO_2 concentrations can be observed during the lockdown period. During this time, concentrations fall below the expected seasonal cycle. Although this behavior was also observed in 2022 and 2023.

It is observable that the time series follows the seasonal cycle, with some significant deviations and sharp peaks. The extreme peak observed in early 2021 suggests a strong rebound effect or the influence of episodic emission sources, such as industrial activity or energy production, which are not tied to mobility restrictions. Overall, while the lockdown measures led to a noticeable reduction in SO_2 concentrations, the variability observed in subsequent periods indicates that SO_2 dynamics are strongly associated with emission sources rather than purely seasonal or mobility related factors.

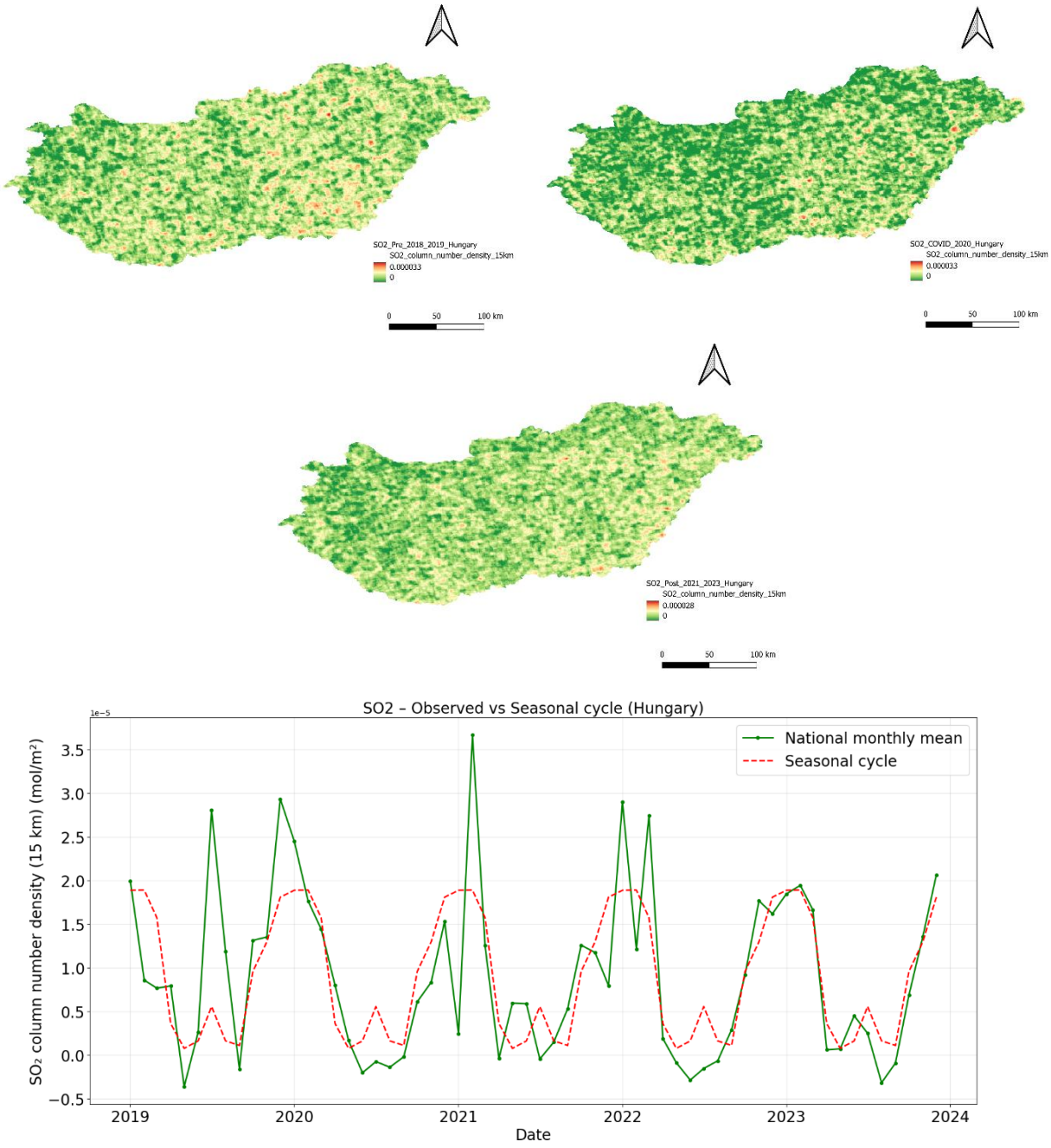

Figure 6: SO_2 Pre-pandemic, Pandemic and Post-pandemic variability and seasonal cycle in Hungary
Source: Own elaboration

As seen in *Figure 7*, for NO_2 the peak concentration was observed in January 2019, and the lowest concentration occurred in November 2020. Considering that COVID-19 restrictions in Hungary began on March 11, 2020, a noticeable reduction in NO_2 concentrations can be observed throughout the year 2020. Compared with both the preceding and following years, 2020 presents the lowest overall concentrations in the time series. During the lockdwon the

observed concentratios fall consistently below the expected seasonal cycle, indicating a reduction beyond normal seasonal variability. This suggests that mobility restrictions had a strong impact.

Furthermore, the overall downward shift in 2020 relative to other years reflects a sustained reduction in emissions during the pandemic, rather than a short-term fluctuation. After 2020, concentrations begin to recover and return close to the seasonal baseline, indicating a gradual resumption of economic activity and mobility patterns.

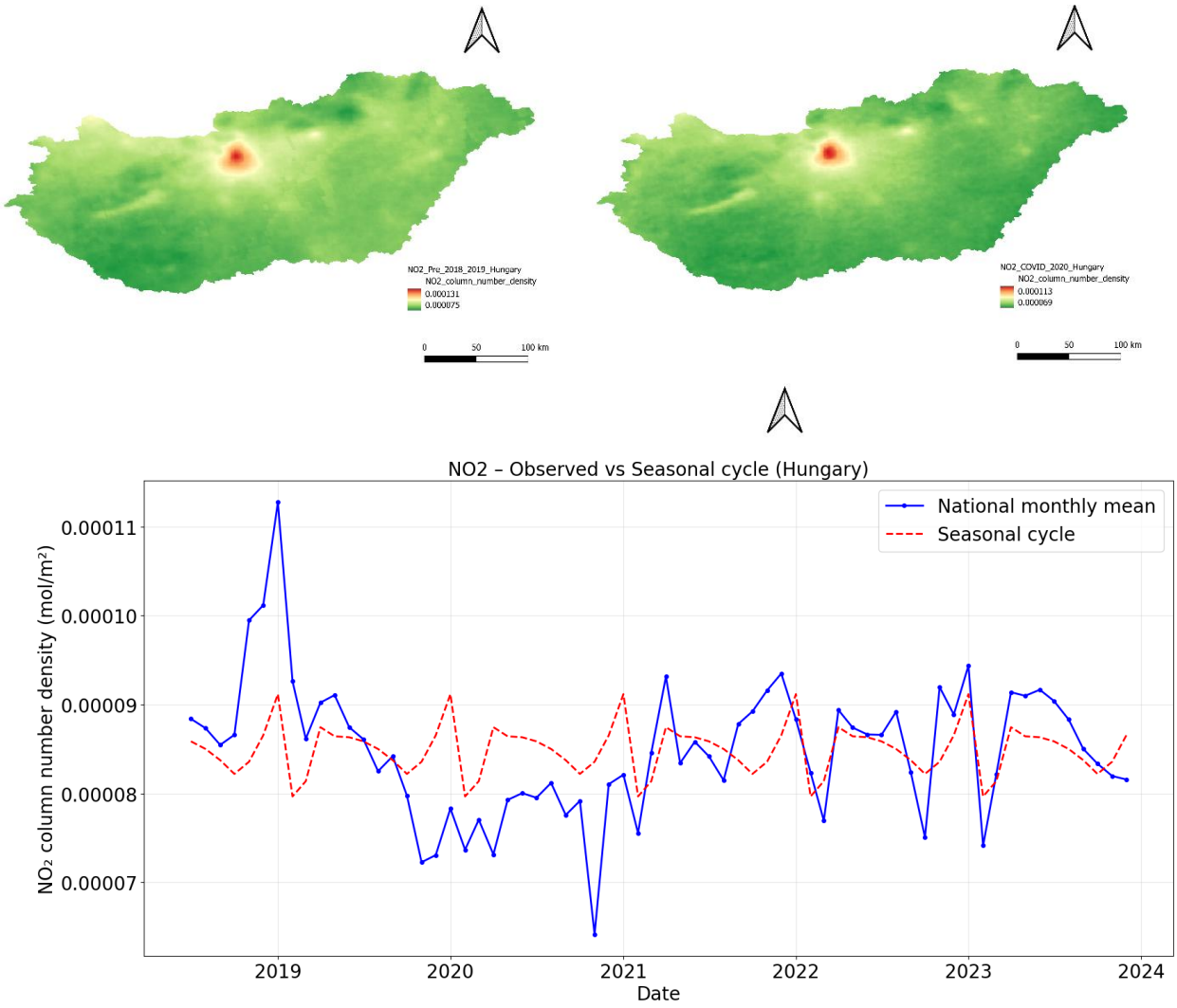

Figure 7: NO_2 Pre-pandemic, Pandemic and Post-pandemic variability and seasonal cycle in Hungary
Source: Own elaboration

As seen in *Figure 8* for CO the peak concentration was observed in July 2021, while the lowest concentration occurred in October 2022. Considering that COVID-19 restrictions in Hungary began on March 11, 2020, a noticeable reduction in CO concentrations can be observed during 2020. This reduction is particularly evident when comparing the typical seasonal pattern observed in other years. Under normal conditions, CO concentrations tend to decrease gradually from spring to summer. However, in 2020, this decline is more abrupt, keeping the concentrations under the expected seasonal pattern. Interestingly, an even stronger reduction is observed in 2022, where concentrations drop more sharply and reach the lowest values in the entire time series.

Overall, CO exhibits a clear seasonal cycle, closely following the expected pattern throughout most of the time series. However, deviations from this cycle particularly during 2020 and 2022 highlight the influence of external drivers beyond seasonal variability

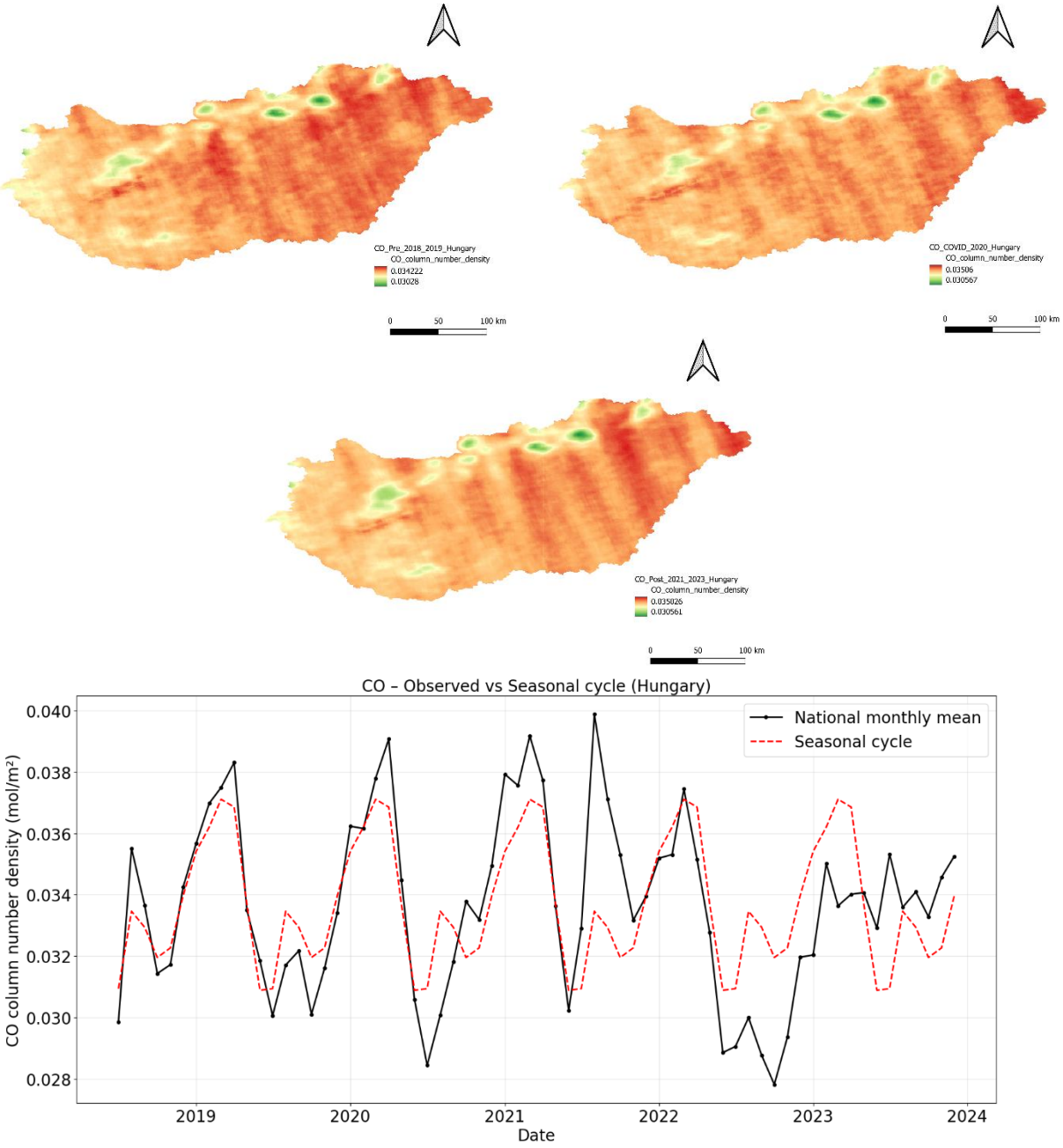

Figure 8: CO Pre-pandemic, Pandemic and Post-pandemic variability and seasonal cycle in Hungary
Source: Own elaboration

4.2. Geospatial and statistical comparison of atmospheric pollutant concentrations (CO, NO_2 and SO_2) before, during and after the COVID-19 pandemic in major Hungarian cities

As *Figure 9* shows, all analyzed cities present similar concentrations of carbon monoxide across the three studied periods. In general, an increase in concentration can be observed during the pandemic period, followed by a decrease during the post-pandemic period.

In Budapest, the pre-pandemic concentration was 0.0340 mol/m², while during the pandemic it increased to 0.0370 mol/m² (+9.03%) In the post-pandemic period, the concentration decreased to 0.0335 mol/m² (−9.45% compared to the pandemic period).In Debrecen, the pre-pandemic concentration was 0.0336 mol/m², increasing during the pandemic to 0.0375 mol/m² (+11.49%). During the post-pandemic period, the value decreased again to 0.036 mol/m² (−10.26%). In Szeged, a similar pattern was observed. The pre-pandemic concentration was 0.0337 mol/m², increasing during the pandemic to 0.0377 mol/m² (+11.68%). In the post-pandemic period, the concentration decreased to 0.0337 mol/m² (−10.52%). Overall, the results show that CO concentrations were higher during the pandemic period in all three cities, while post-pandemic levels returned to values like those observed before the pandemic.

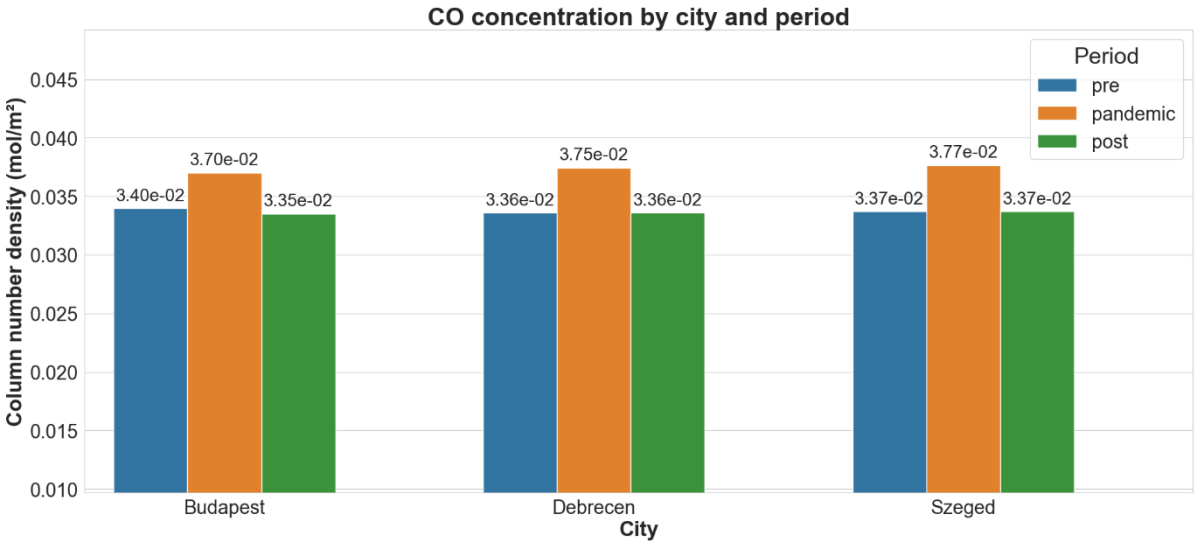

CO concentration comparison by city

city	pre	pandemic	post	pandemic_change_%	post_change_%
Budapest	3.40e-02	3.70e-02	3.35e-02	9.029	-9.454
Debrecen	3.36e-02	3.75e-02	3.36e-02	11.489	-10.262
Szeged	3.37e-02	3.77e-02	3.37e-02	11.678	-10.519

Figure 9: CO concentration by city and period
Source: Own elaboration

As *Figure 10* shows, nitrogen dioxide concentrations show a general decrease during the pandemic period in all analyzed cities.

In Budapest, the pre-pandemic concentration was 0.000069 mol/m², decreasing during the pandemic to 0.000061 mol/m² (−11%). In the post-pandemic period, the concentration increased again to 0.000066 mol/m² (+8.6% compared to the pandemic period).

In Debrecen, the pre-pandemic concentration was 0.000032 mol/m², decreasing during the pandemic to 0.000029 mol/m² (−11.58%). In the post-pandemic period, the concentration slightly recovered to 0.000032 mol/m² (+11.5%).

In Szeged, the pre-pandemic concentration was 0.000033 mol/m², decreasing during the pandemic to 0.000028 mol/m² (−15.3%). In the post-pandemic period, the concentration increased again to 0.000032 mol/m² (+15.1%).

These results indicate that NO_2 experienced a general reduction during the pandemic, followed by a partial recovery in the post-pandemic period.

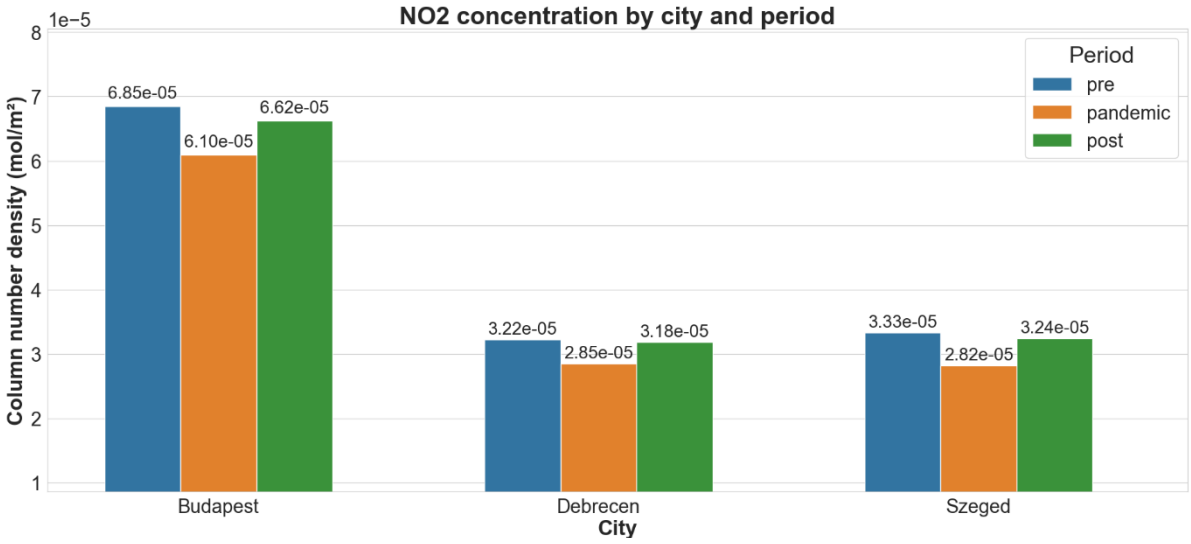

NO2 concentration comparison by city

city	pre	pandemic	post	pandemic_change_%	post_change_%
Budapest	6.85e-05	6.10e-05	6.62e-05	-11.003	8.615
Debrecen	3.22e-05	2.85e-05	3.18e-05	-11.583	11.550
Szeged	3.33e-05	2.82e-05	3.24e-05	-15.258	15.099

Figure 10: NO_2 concentration by city and period
Source: Own elaboration

As *Figure 11* shows, sulfur dioxide concentrations show greater spatial variability among the cities analyzed, although overall values remain relatively low.

In Budapest, the pre-pandemic concentration was 0.00000764 mol/m², decreasing during the pandemic to 0.00000533 mol/m² (−30.2%). In the post-pandemic period, the concentration increased to 0.000006 mol/m² (+20.1% compared to the pandemic period), although it remained below pre-pandemic levels.

In Debrecen, the pre-pandemic concentration was 0.00000968 mol/m², slightly increasing during the pandemic to 0.0000101 mol/m² (+4.41%). In the post-pandemic period, the concentration decreased to 0.00000771 mol/m² (−23.77%).

In Szeged, the pre-pandemic concentration was 0.0000144 mol/m², increasing during the pandemic to 0.0000148 mol/m² (+2.62%). In the post-pandemic period, the concentration decreased significantly to 0.000008 mol/m² (−44.52%).

Overall, SO_2 concentrations remained relatively low across all cities, with moderate variations between the analyzed periods.

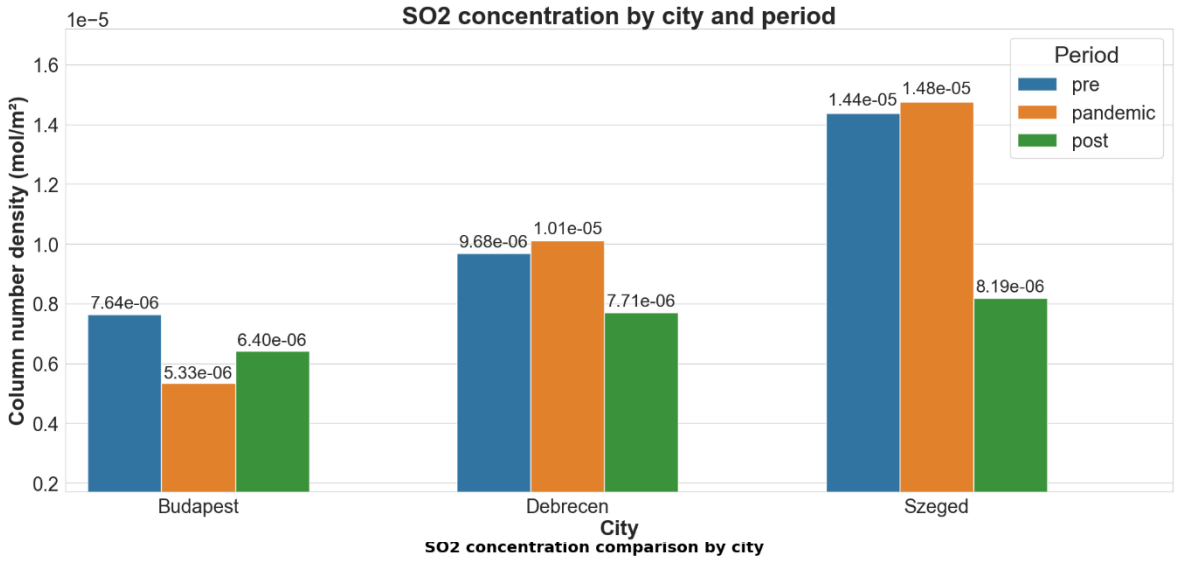

SO2 concentration comparison by city

city	pre	pandemic	post	pandemic_change_%	post_change_%
Budapest	7.64e-06	5.33e-06	6.40e-06	-30.194	20.081
Debrecen	9.68e-06	1.01e-05	7.71e-06	4.408	-23.765
Szeged	1.44e-05	1.48e-05	8.19e-06	2.622	-44.521

Figure 11: SO_2 concentration by city and period
Source: Own elaboration

T
inverse seasonal pattern, with a Pearson correlation coefficient of r = -0.490, indicating a

moderate negative correlation, meaning CO concentrations tend to decrease as temperature increases.

This behavior is consistent with the seasonal dynamics of CO emissions. During colder periods, increased residential heating and combustion processes lead to higher CO concentrations, while stable atmospheric conditions limit pollutant dispersion. In contrast, warmer periods are associated with reduced heating demand, enhanced atmospheric mixing, and increased photochemical oxidation, all of which contribute to lower CO levels.

The moderate strength of the correlation suggests that temperature is not the sole driver of CO variability. Deviations from the expected seasonal pattern indicate the influence of additional factors, such as traffic emissions, energy consumption, and other anthropogenic activities.

For CO, during the pandemic period (March–May 2020), a slight decrease in concentrations can be observed in the time series, although the reduction is not as pronounced as in other pollutants. Maximum CO values are recorded during colder periods, particularly around early 2021 and again near early 2022, where the highest peaks are observed. Additional elevated values are also present towards late 2023. In contrast, minimum concentrations occur during warmer months, especially in mid-2020 and mid-2022, where CO reaches its lowest levels. Overall, CO shows a consistent pattern of seasonal variation with clearly identifiable maxima and minima throughout the study period.

Overall, while temperature plays an important role in modulating CO concentrations, the observed variability reflects a combination of climatic and emission-related influences, highlighting the complex behavior of CO in urban environments (*Figure 12)*.

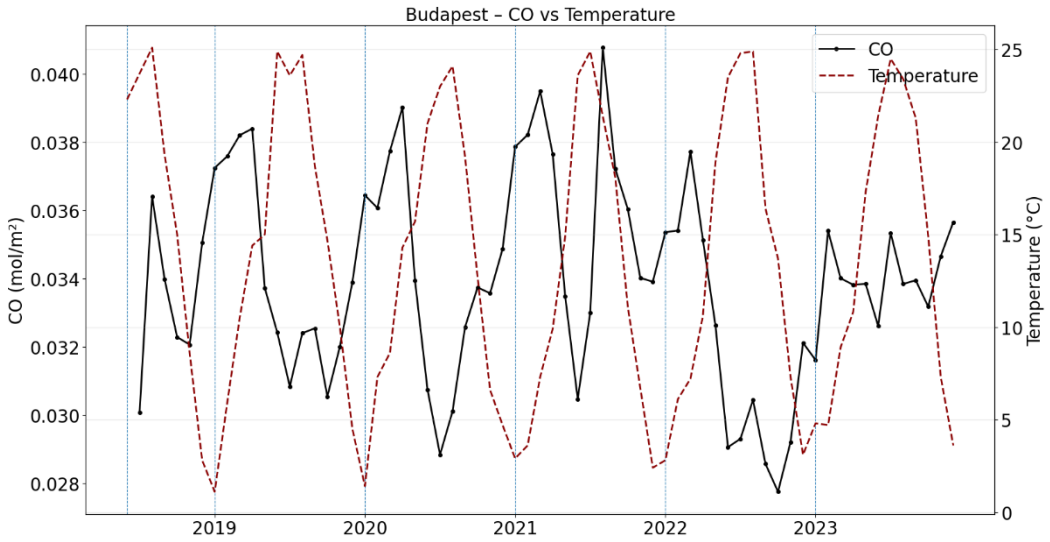

Figure 12: CO vs Temperature in Budapest
Source: Own elaboration

The relationship between NO_2 and SO_2 concentrations with temperature in Budapest reveals distinct behaviors for each pollutant, supported by their respective Pearson correlation coefficients.

NO_2 exhibits a strong inverse relationship with temperature, with a Pearson correlation coefficient of r = -0.811. This indicates a strong negative correlation, confirming that NO_2 concentrations decrease significantly as temperature increases. This behavior reflects the strong influence of seasonal and temperature-dependent processes, including increased emissions from traffic and heating during colder months, as well as reduced atmospheric dispersion.

For NO_2, a noticeable decrease is evident during the pandemic period (March–May 2020), with lower values compared to surrounding months. NO_2 reaches its maximum concentrations during colder periods, with prominent peaks observed around early 2019, early 2021, and especially early 2022, representing the highest values in the dataset. Elevated concentrations are also visible in 2023. Minimum values consistently occur during warmer periods, particularly in summer months, where NO_2 concentrations reach their lowest levels. The temporal pattern shows clear and repeated fluctuations with well-defined peaks and troughs *(Figure 13)*.

In contrast, SO_2 shows a weaker and more irregular relationship with temperature, with a Pearson correlation coefficient of r = -0.524. This moderate negative correlation suggests that, while temperature has some influence on SO_2 variability, it is not the dominant controlling factor. The presence of sporadic peaks and high variability in the time series indicates that SO_2 is more strongly affected by episodic or localized emission sources.

For SO_2, the pandemic period (March–May 2020) does not show a clear or consistent reduction, and concentrations remain highly variable. SO_2 exhibits irregular behavior across the time series, with several pronounced peaks that do not follow a consistent seasonal pattern. The highest concentrations are observed around early 2019 and early 2021, with additional peaks occurring in 2022 and 2023. In contrast, minimum values appear intermittently throughout the series, including multiple periods where concentrations are close to zero. Overall, SO_2 displays a highly variable pattern characterized by sporadic maxima and irregular minima over time (*Figure 13*).

Overall, the comparison highlights that NO_2 is strongly driven by seasonal and temperature-related factors, whereas SO_2 exhibits a more complex behavior influenced by additional non-seasonal emission sources.

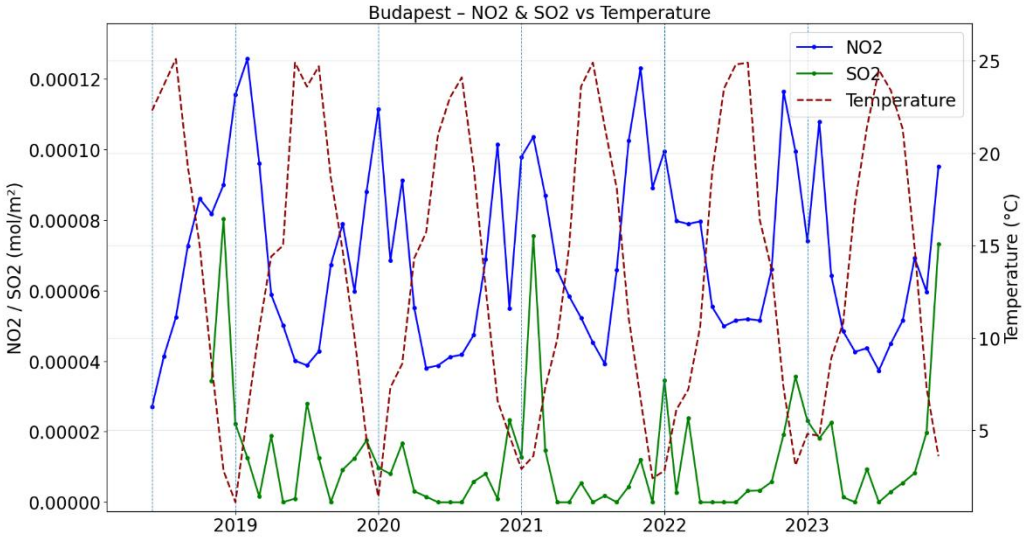

Figure 13. NO_2 and SO_2 vs Temperature in Budapest
Source: Own elaboration

The relationship between CO concentrations and temperature in Szeged shows a clear inverse seasonal pattern, supported by a Pearson correlation coefficient of r = -0.444. This

value indicates a moderate negative correlation, meaning that CO concentrations tend to decrease as temperature increases.

This behavior is consistent with the seasonal dynamics of CO emissions. Higher concentrations are observed during colder months, when residential heating and combustion-related activities increase, and atmospheric conditions favor pollutant accumulation due to reduced mixing and dispersion. In contrast, during warmer periods, lower CO concentrations are associated with decreased heating demand, enhanced atmospheric mixing, and increased photochemical oxidation.

The moderate strength of the correlation suggests that temperature plays an important, but not exclusive, role in controlling CO variability in Szeged. Overall, the results for Szeged are consistent with those observed in Budapest, confirming that CO is partially driven by temperature while also being influenced by a combination of anthropogenic and atmospheric processes.

For CO, during the pandemic period (March–May 2020), a slight reduction in concentrations can be observed in the time series. However, this decrease is relatively moderate compared to other pollutants. The highest CO concentrations are recorded during colder periods, particularly around early 2021 and again near early 2022, where peak values are evident. In contrast, the lowest concentrations occur during warmer periods, especially in mid-2020 and mid-2022, where CO reaches its minimum levels. Overall, CO displays a clear seasonal fluctuation with identifiable maxima and minima throughout the study period *(Figure 14)*.

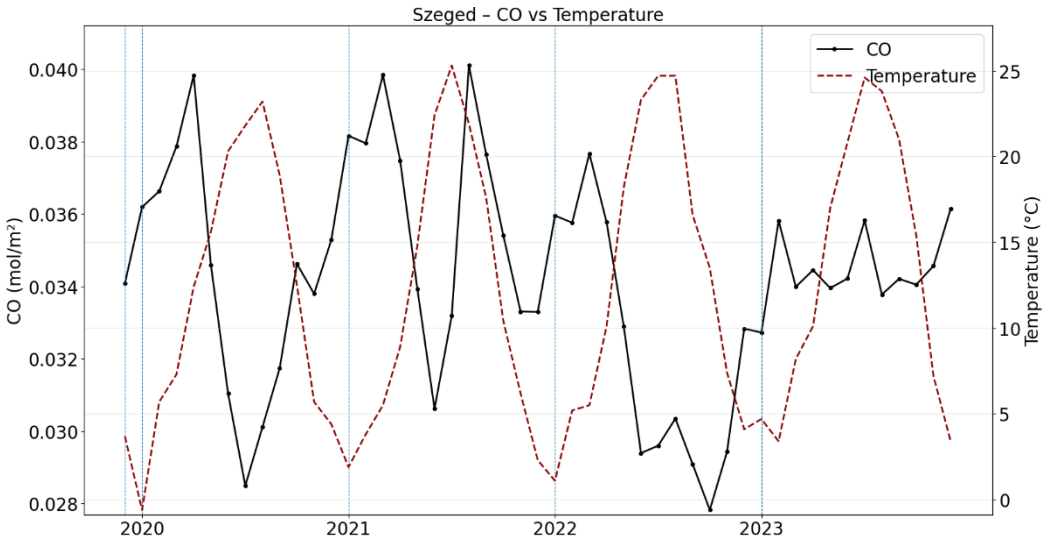

Figure 14. CO vs Temperature in Szeged
Source: Own elaboration

The relationship between NO_2 and SO_2 concentrations with temperature in Szeged reveals distinct patterns for each pollutant, supported by their respective Pearson correlation coefficients.

NO_2 exhibits a strong inverse relationship with temperature, with a Pearson correlation coefficient of r = -0.740. This indicates a strong negative correlation, meaning that NO_2 concentrations decrease significantly as temperature increases. The seasonal pattern is clearly defined, with higher concentrations during colder months due to increased emissions from traffic and heating, combined with reduced atmospheric dispersion, and lower concentrations during warmer periods driven by enhanced mixing and photochemical processes.

For NO_2, a noticeable decrease is observed during the pandemic period (March–May 2020), reflected by lower concentration values compared to adjacent months. NO_2 presents well-defined maximum values during colder periods, with prominent peaks occurring around early 2021 and especially early 2022, where the highest concentrations in the time series are recorded. Additional elevated values are also visible towards late 2023. Minimum concentrations consistently occur during warmer months, particularly in summer periods, where NO_2 reaches its lowest levels. The temporal pattern shows clear variability with distinct peaks and troughs across the study period *(Figure 15)*.

In contrast, SO_2 shows a moderate negative correlation with temperature, with a Pearson correlation coefficient of r = -0.627. While this suggests that temperature does influence

SO_2 concentrations to some extent, the relationship is less consistent than for NO_2. The time series displays notable variability and sporadic peaks that do not always align with the seasonal temperature pattern, indicating the influence of additional factors such as localized or episodic emission sources.

Overall, the results indicate that NO_2 in Szeged is strongly controlled by seasonal and temperature-related processes, whereas SO_2 exhibits a more complex behavior influenced by both climatic conditions and irregular emission sources. These findings are consistent with those observed in other cities, reinforcing the pollutant-specific nature of air quality dynamics.

For SO_2, the pandemic period (March–May 2020) does not show a clear or consistent reduction in concentrations, and values remain variable. SO_2 exhibits significant fluctuations throughout the time series, with pronounced peaks that stand out from the general pattern. The highest concentrations are observed around early 2022, representing the most notable peak in the dataset, as well as additional elevated values in 2023. In contrast, minimum values occur intermittently across different periods, including several months when concentrations approach near-zero levels. Overall, SO_2 displays a highly variable behavior with irregular maxima and minima over time*(Figure 15)*.

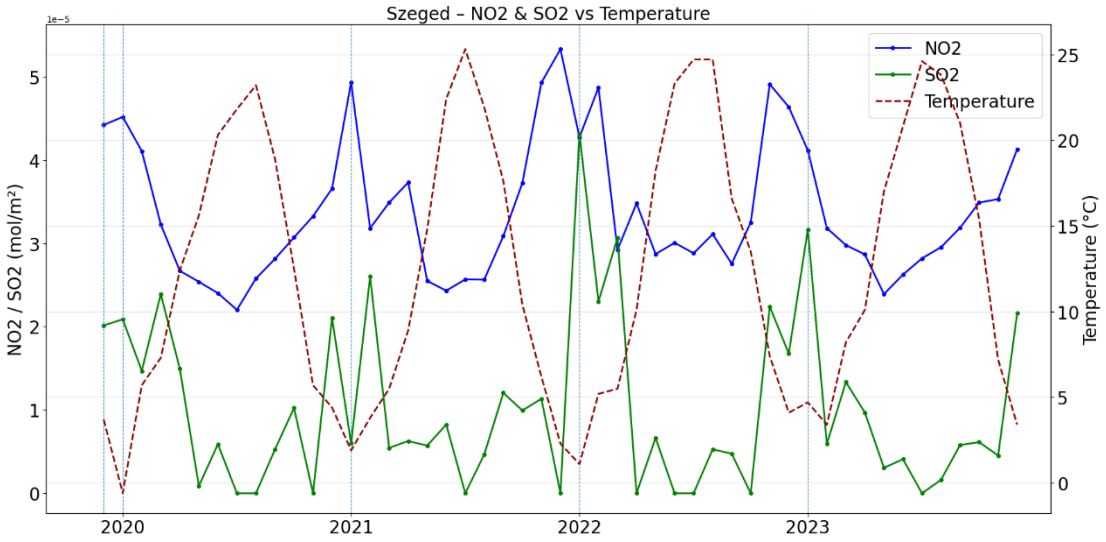

Figure 15. NO_2 and SO_2 vs Temperature in Szeged
Source: Own elaboration

The relationship between CO concentrations and temperature in Debrecen shows a clear inverse seasonal pattern, supported by a Pearson correlation coefficient of r = -0.46. This value indicates a moderate negative correlation, suggesting that CO concentrations tend to decrease as temperature increases. This is evident in the time series, where higher CO values consistently coincide with colder periods, while lower concentrations are observed during warmer months.

This behavior reflects the seasonal dynamics of CO emissions and atmospheric processes. During colder months, increased residential heating and combustion-related activities contribute to higher CO emissions. In contrast, warmer periods are characterized by lower CO concentrations due to reduced heating demand and atmospheric processes.

During the pandemic period, a slight decrease in concentrations can be observed, consistent with the reduction in mobility and combustion related activities. CO emissions are influenced not only by traffic but also by residential heating and other sources that remained active during lockdowns. The highest CO concentrations are generally observed during colder months, particularly in winter periods such as late 2021, when heating demand increases and atmospheric dispersion is limited. In contrast, the lowest CO values occur during warmer months, especially in summer, when enhanced atmospheric mixing and reduced emissions contribute to lower concentrations *(Figure 16)*.

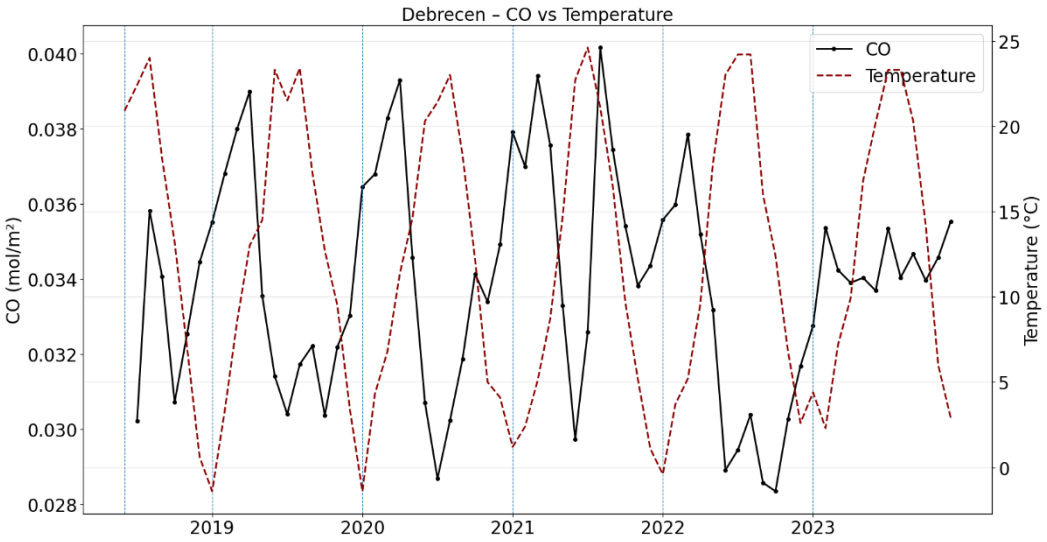

Figure 16. CO vs Temperature in Debrecen
Source: Own elaboration

The relationship between NO_2 and SO_2 concentrations with temperature in Debrecen reveals distinct behaviors for each pollutant, supported by their Pearson correlation coefficients.

NO_2 exhibits a strong inverse relationship with temperature, with a Pearson correlation coefficient of r= -0.70, indicating a strong negative correlation, meaning that NO_2 concentrations decrease significantly as temperature increases. The seasonal pattern is clearly defined in the time series, with elevated concentrations during colder months. In contrast, during warmer periods, lower NO_2 concentrations are observed.

For NO_2, a more pronounced reduction in evident during the pandemic period, reflecting its strong dependence on traffic related emissions. The decrease in during this period highlights the direct impact of mobility restrictions on NO_2 levels. Maximum concentrations are observed during colder seasons, with a notable peak around late 2021, likely associated with increased traffic activity and reduced atmospheric dispersion. Minimum concentrations are consistently recorded during warmer months *(Figure 17)*.

In contrast, SO_2 shows a moderate negative correlation with temperature, with a Pearson correlation coefficient of r=-0.52, this suggests that temperature plays a role in influencing SO_2, but the relationship is less consistent compared to NO_2. The temporal evolution of SO_2 displays considerable variability, including sporadic peaks that do not always coincide with seasonal temperature patterns, indicating that other factors influence the concentrations.

For SO_2, the impact of the pandemic period is less clearly defined compared to CO and NO_2, indicating a weaker link to traffic related emissions. SO_2 concentrations exhibit significant variability throughout the time series, with several pronounced peaks that do not strictly follow seasonal patterns. Strong peaks are observed in late 2021 and 2023. Minimum values are generally observed during warmer periods *(Figure 17)*.

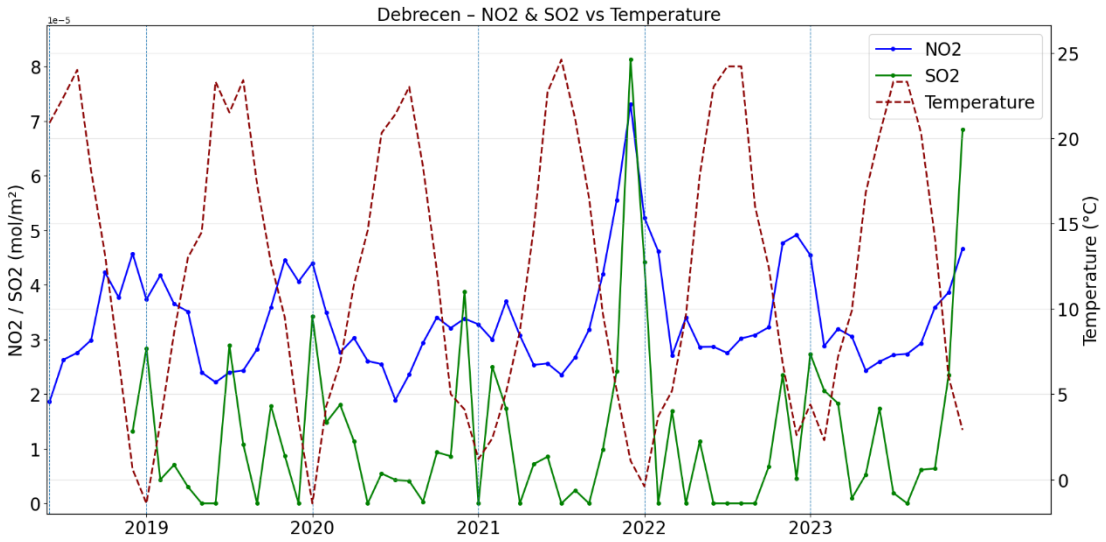

Figure 17. NO_2 and SO_2 vs Temperature in Debrecen
Source: Own elaboration

5. DISCUSSION

5.1. Pollutant seasonal patterns and concentrations

Clear seasonal pollutant patterns were observed from CO, NO_2 and SO_2. Pollutants showed a clear rising tendency during cold months and an abrupt decrease during warmer months, these tendencies are strongly associated with anthropogenic activities.

The temporal variations of the pollutants show that each pollutant responded differently to the COVID-19 period, while still maintaining the overall seasonal pattern. Among the three, NO_2 showed the most pronounced decline during 2020, with the lowest concentration recorded in November 2020 and its concentration consistently remaining below the expected seasonal cycle during the whole year. This sustained reduction suggests a clear disruption in the typical emission dynamics showing a strong relationship between the pollutant and traffic related emisions. From 2021 concentrations gradually increased until surpassed the pre-pandemic levels which can be interpreted as a rebound effect, as Jean-Philippe Putaud et al. (2023) found in their investigation too. NO_2 shows consistent and well-defined response across all cities, with a clear decrease during the pandemic period followed by a partial recovery afterward. Reduction values were: -11% for Budapest, -11.58% for Debrecen and -15.26% for Szeged, showing coherence with the study carried out by Pieternel F. Levelt et al. (2022), where they determined that the reduction range is

between -14% and -63% for megacities all over the world. The author also emphasized that this pollutant is highly influenced by transportation.

CO also presented a decrease during 2020, although less pronounced e compared to NO_2. The time series shows that CO generally follows a stable seasonal pattern; however, during the lockdown period (March-May 2020) the decline appears more abrupt than previous years indicating a deviation from normal conditions. In addition, a more pronounced reduction is observed in 2022, when CO reaches its lowest value in the entire time series. This suggests that factors beyond the pandemic contributed to this behavior, reinforcing the idea that CO variability is influenced by multiple factors.

In a national scale, the CO concentrations showed a slight decrease, coinciding with the study of Gabriela Cioca & Raluca Andreea Nerișanu (2022), where they showed the reduction of the concentrations were up to -25% in Hungary. Although the difference in the magnitudes is due to the way the periods were established and the satellite used for the study.

In a city scale and in contrast to expectations, CO concentrations increased during the pandemic period in the three analyzed cities. The increase during the lockdown period could be attributed to industries, power plants and indoor activities like heaters engaged in cooking, heating and smoking (Manisalidis et al., 2020).

SO_2 in contrast, displays a markedly different pattern characterized by high variability and less consistent behavior. A decrease is observed during the lockdown period, but it is not as clear or as sustained as in NO_2. The most notable feature of the SO_2 time series is the pronounced peak observed in February 2021, which represents a significant variation from the seasonal pattern. Additional fluctuations are observed in the subsequent years further highlighting the irregular nature of this pollutant, meaning that its temporal evolution is not strictly influenced by seasonal or pandemic related changes.

In a city scale, SO_2 also exhibits a more heterogeneous behavior, indicating a weaker and less uniform response to the pandemic. In contrast to expectations, Budapest shows a clear decrease during the lockdown period, Debrecen and Szeged present slight increases, followed by reductions in the post pandemic period, which coincides with the study of Gabriela Cioca & Raluca Andreea Nerișanu (2022), where they found that SO_2 suffered a reduction of 8.38% in ground level emissions. This shows that SO_2 concentrations are not

only influenced by mobility restrictions but also power plants and other fossil fuel sources, along with oil refineries and natural gas refineries, reported a reduction in activity based on general energy demand reduction (Reddy & Venkataraman, 2002).

When comparing the three pollutants, it becomes evident that their responses to external disturbances differ in magnitude and consistency. NO_2 shows the strongest response, with a clear reduction during 2020. CO shows a moderate response, maintaining its seasonal structure, but showing important deviations during some months. In contrast, SO_2 demonstrates a weaker and less clear response.

Despite these differences, all three pollutants share a general tendency to get higher during colder months and lower values during warmer months. NO_2 shows the most clearly defined cycle, followed by CO and finally SO_2. Indicating that, although seasonality is an important factor, it does not affect all pollutants equally.

5.2. Pollutants and temperature

Results show there is a relationship between temperature and pollutant concentration. Among all the pollutants, NO_2 shows the most consistent and pronounced negative correlation with the temperature, it also shows a clear reduction during 2020, confirming the influence of traffic and urban mobility. In contrast, CO exhibits a more complex response, characterized by a moderate correlation with temperature and a less pronounced reduction during the pandemic period. The persistence of relatively high CO concentrations during the pandemic period suggests that its emissions are not exclusively linked to mobility. Instead, the results indicate that other sources such as residential heating and energy consumption likely played a significant role in maintaining CO levels. The additional decrease observed in 2022, in the absence of pandemic restrictions, further supports the idea that CO variability is influenced by a combination of meteorological conditions and changes in emission patterns, rather than a single dominant driver.

SO_2 presents a distinct behavior compared to the other pollutants. A noticeable reduction during the pandemic period is observed, indicating that SO_2 emissions were affected by the decrease in anthropogenic activities. However, unlike NO_2 this reduction is not accompanied by a clear correlation between SO_2 and temperature, this weak correlation indicates that the concentrations are not controlled by seasonal atmospheric processes. Instead, the presence of pronounced peaks and fluctuations throughout the time series

indicates that SO_2 is more influenced by emission intensity and episodic sources rather than temperature driven dynamics.

Additionally, the correlation with temperature indicates that seasonal dynamics play an important role in modulating pollutant concentrations, although not uniformly across pollutants. While NO_2 shows a strong dependence on temperature and CO a moderate one, SO_2 deviates from this pattern, showing why temperature is not the only influencing the pollutant concentration.

6. CONCLUSIONS

Air pollutant concentrations in Hungary follows a strong seasonal pattern, with higher values during colder months and lower concentrations during warmer periods, reflecting the influence of anthropogenic activities such as heating and energy consumption. However, COVID-19 pandemic introduced a clear variation in these typical dynamics, affecting each pollutant in a different way.

NO_2 showed the most consistent and pronounced response to the lockdown measures. A significant decrease was observed during 2020 across all cities, highlighting its strong association with traffic related emissions and urban mobility. A rebound effect linked to the resumption of economic and transportation activities could be witnessed in 2021.

CO exhibited a more complex and less uniform behavior. Although a general decrease was observed during 2020, the persistence of relatively high concentrations, particularly at a city scale, shows that its emissions are not exclusively dependent on traffic. Instead, residential heating, energy consumption and production, and other combustion related activities might play a significant role. The additional decrease observed in 2022 further highlights that CO variability is influenced by multiple factors, including emission sources and meteorological conditions.

SO_2 displayed the highest variability and the weakest response to lockdown measures. While a slight decrease was observed during the pandemic period, its temporal evolution was characterized by irregular fluctuations and a pronounced peak in early 2021.

Overall, the results highlight that the impact of COVID-19 restrictions on air quality was pollutant specific and strongly dependent on emission sources. While traffic related

pollutants such as NO_2 responded clearly to mobility reductions, pollutants associated with stationary sources such as SO_2 and CO, showed more complex behaviors.

This study demonstrates the value of satellite observations, particularly Sentinel-5P TROPOMI data, for capturing large scale temporal variations in air pollutants and identifying differences in pollutant behavior across urban environments. These findings contribute to a better understanding of emission dynamics.

7. BIBLIOGRAPHY

Ackerman, S., & Knox, J. (2007). *Meteorology : understanding the atmosphere* ((CA: Thoms).

Alvarez, C. I. (2014). Estimación De Contaminación Del Aire Por Pm10 En Quito Determinado Por Indices Ambientales Obtenidos Con Imágenes Satelitales Landsat Etm+. *Vicerrectorado de Investigación y Vinculación Con La Colectivida*, *53*, 104. http://repositorio.espe.edu.ec/bitstream/21000/8675/1/T-ESPE-047962.pdf

Atkinson, R.W., et al., 2018. Long-term concentrations of nitrogen dioxide and mortality: a meta-analysis of cohort studies. Epidemiology 29 (4), 460–472.

Bentayeb, M., et al., 2015. Association between long-term exposure to air pollution and mortality in France: a 25-year follow-up study. Environ. Int. 85, 5–14.

Blomberg, A., Krishna, M. T., Helleday, R., Söderberg, M., Ledin, M. C., Kelly, F. J., Frew, A. J., Holgate, S. T., & Sandström, T. (1999). Persistent airway inflammation but accommodated antioxidant and lung function responses after repeated daily exposure to nitrogen dioxide. American Journal of Respiratory and Critical Care Medicine, 159(2), 536–543. https://doi.org/10.1164/ajrccm.159.2.9711068

Chen, T. M., Gokhale, J., Shofer, S., & Kuschner, W. G. (2007). Outdoor air pollution: Nitrogen dioxide, sulfur dioxide, and carbon monoxide health effects. American Journal of the Medical Sciences, 333(4), 249–256. https://doi.org/10.1097/MAJ.0b013e31803b900f

Cioca, G., & Nerișanu, R. A. (2022). The effects of pandemic restrictions on public health—Improvements in urban air quality. International Journal of Environmental Research and Public Health, 19(14), 9022. https://doi.org/10.3390/ijerph19149022

Delon, S. (2018). La Pollution de l'air: sources, effets, prévention [Air pollution: sources, effects, prevention]. APPA (Association pour la Prévention de la Pollution Atmosphérique).

Earth Engine Data Catalog. (2018). Sentinel collections in Earth Engine | Earth Engine Data Catalog. Sentinel Collection. https://developers.google.com/earthengine/datasets/catalog/sentinel-5p

Eskes, H., van Geffen, J., Boersma, F., Eichmann, K.-U., Apituley, A., Pedergnana, M., Sneep, M., Veefkind, J. P., & Loyola, D. (2021). *Sentinel-5 precursor / TROPOMI Level 2 Product User Nitrogen Dioxide*. *4.1.0*, 128. https://sentinel.esa.int/web/sentinel/ technical-guides/sentinel-5p/

García, A. (2000). *LANDSAT*. 2–40.

Gul, H., & Das, B. K. (2023). The Impacts of Air Pollution on Human Health and Well-Being: A Comprehensive Review. Journal of Environmental Impact and Management Policy, (36), 1–11. https://doi.org/10.55529/jeimp.36.1.11.

Haq, G., & Schwela, D. (2008). *Urban air pollution in Asia: A framework for action*. Stockholm Environment Institute.

Hasselblad, V., Eddy, D. M., & Kotchmar, D. J. (1992). Synthesis of environmental evidence: Nitrogen dioxide epidemiology studies. Journal of Air Waste Management Association, 42(6), 662–671.

Heilig, G. K. (1994). The greenhouse gas methane (CH4): Sources and sinks, the impact of population growth, possible interventions. *Population and Environment*, *16*(2), 109–137. https://doi.org/10.1007/BF02208779

Huang, S., Li, H., Wang, M., Qian, Y., Steenland, K., Caudle, W. M., … Shi, L. (2021). Long-term exposure to nitrogen dioxide and mortality: A systematic review and meta-analysis. Science of the Total Environment, 776, 145968. https://doi.org/10.1016/j.scitotenv.2021.145968

Hungarian Geographical Institute. (2012). Hungary in the world: Geographical location and geopolitical situation. https://hungarian-geography.hu/inmaps/pdf/Hungary-in-Maps_9.pdf

Khalaf, E. M., Mohammadi, M. J., Sulistiyani, S., Ramírez-Coronel, A. A., Kiani, F., Jalil, A. T., … Derikondi, M. (2024). Effects of sulfur dioxide inhalation on human health: A review. Reviews on Environmental Health, 39(2), 331–337. https://doi.org/10.1515/reveh-2022-0237

Liu, F., et al., 2019. Associations between long-term exposure to ambient air pollution and risk of type 2 diabetes mellitus: a systematic review and meta-analysis. Environ. Pollut. 252 (Pt B), 1235–1245.

Lillesand, T. M., Kiefer, R. W., & Chipman, J. W. (2015). Remote sensing and image interpretation. In *Australian Journal of Geodesy, Photogrammetry & Surveying* (7th editio, Vol. 39). Wiley. https://www.geokniga.org/bookfiles/geokniga-remote-sensing-and-image-interpretation.pdf

Levelt, P. F., Stein Zweers, D. C., Aben, I., Bauwens, M., Borsdorff, T., De Smedt, I., Eskes, H. J., Lerot, C., Loyola, D. G., Romahn, F., Stavrakou, T., Theys, N., Van Roozendael, M., Veefkind, J. P., & Verhoelst, T. (2022). Air quality impacts of COVID-19 lockdown measures detected from space using high spatial resolution observations of multiple trace gases from Sentinel-5P/TROPOMI. Atmospheric Chemistry and Physics, 22, 10911–10937. https://doi.org/10.5194/acp-22-10911-2022

Manisalidis, I., Stavropoulou, E., Stavropoulos, A., & Bezirtzoglou, E. (2020). Environmental and health impacts of air pollution: A review. Frontiers in Public Health, 8, 14. https://doi.org/10.3389/fpubh.2020.00014

Olaya, V. (2014). *Sistemas de Información Geográfica*. 854.

Onursal, B., & Gautam, S. P. (1984). Contaminantes del aire y sus efectos. *Paper*, *2*(1), 43. http://documentacion.ideam.gov.co/openbiblio/bvirtual/001083/Course2/Lecturas/Vehiculos/chapter2.pdf

Pénard-Morand, C., & Annesi-Maesano, I. (2004). Air pollution: from sources of emissions to health effects. Epidemiology of Allergic and Respiratory Diseases (EPAR), 375–394. https://doi.org/10.1142/9789814366984_0022

Putaud, J.-P., Pisoni, E., Mangold, A., Hueglin, C., Sciare, J., Pikridas, M., Savvides, C., Ondracek, J., Mbengue, S., Wiedensohler, A., Weinhold, K., Merkel, M., Poulain, L., van Pinxteren, D., Herrmann, H., Massling, A., Nordstroem, C., Alastuey, A., Reche, C., Pérez, N., Castillo, S., Sorribas, M., Adame, J. A., Petaja, T., Lehtipalo, K., Niemi, J., Riffault, V., de Brito, J. F., Colette, A., Favez, O., Petit, J.-E., Gros, V., Gini, M. I., Vratolis, S., Eleftheriadis, K., Diapouli, E., Denier van der Gon, H., Yttri, K. E., & Aas, W. (2023). Impact of 2020 COVID-19 lockdowns on particulate air pollution across Europe. Atmospheric Chemistry and Physics, 23, 12345–12378. https://doi.org/10.5194/acp-23-12345-2023.

Raub, J. A., & Benignus, V. A. (2002). *Carbon monoxide and the nervous system*.

Neuroscience & Biobehavioral Reviews, 26(8), 925–940. https://doi.org/10.1016/S0149-7634(02)00069-7

Reddy, M. S., & Venkataraman, C. (2002). Inventory of aerosol and sulphur dioxide emissions from India. Part II—Biomass combustion. Atmospheric Environment, 36, 699–712. https://doi.org/10.1016/S1352-2310(01)00464-2

Rice, M., Balmes, J., Malhotra, A., Castner, J., Garcia, E., Hicks, A., Shankar, H., & Sockrider, M. (2021). Outdoor air pollution and your health. *American Journal of Respiratory and Critical Care Medicine*, *204*(7), P13–P14. https://doi.org/10.1164/rccm.2046P13

Sarla, G. S. (2020). Air pollution : Health effects. *Scielo*, *37*(1), 33–38.

Saldiva, P. H., Lichtenfels, A. J., Paiva, P. S., et al. (1994). Association between air pollution and mortality due to respiratory diseases in children in Sao Paulo, Brazil: A preliminary report. Environmental Research, 65(2), 218–225

Shannigrahi, A. S., Fukushuma, T., & Sharma, R. C. (2004). Anticipated air pollution tolerance of some plant species considered for greenbelt development in and around an industrial/urban area in India: An overview. International Journal of Environmental Studies, 61(2), 125–137.

Singh, H. G. (1995). Composition, chemistry, and climate of the atmosphere. *Composition, Chemistry, and Climate of the Atmosphere*. https://doi.org/10.1016/s1352-2310(96)00207-5

Solórzano Villegas, J. V., & Perilla Suárez, G. A. (2022). *Cómo usar Google earth engine (y sobrevivir)*.

Sonwani, S., & Saxena, P. (2021). *Identifying the Sources of Primary Air Pollutants and their Impact on Environmental Health: A Review*. *October 2016*. www.science24.org.

Veefkind, J. P., Aben, I., McMullan, K., Förster, H., de Vries, J., Otter, G., Claas, J., Eskes, H. J., de Haan, J. F., Kleipool, Q., van Weele, M., Hasekamp, O., Hoogeveen, R., Landgraf, J., Snel, R., Tol, P., Ingmann, P., Voors, R., Kruizinga, B., … Levelt, P. F. (2012). TROPOMI on the ESA Sentinel-5 Precursor: A GMES mission for global observations of the atmospheric composition for climate, air quality and ozone layer applications. *Remote Sensing of Environment*, *120*, 70–83.

https://doi.org/https://doi.org/10.1016/j.rse.2011.09.027

Weinstein, L. H. (1977). Fluoride and plant life. Journal of Occupational Medicine, 19(1), 49-78.

WHO. (2010). WHO guidelines for indoor air quality: selected pollutants, 35(8), 812–815. Retrieved from https://iris.who.int/handle/10665/260127

WHO, 2020. Ambient air pollution: health impacts. Available from: https://www.who.int/airpollution/ambient/health-impacts/en/

8. ATTACHMENTS

ANNEX I. Main script for downloading data from Google Earth Engine

```
// ========================================================
// REGIÓN: HUNGRÍA
// ========================================================
var hungary = ee.FeatureCollection("FAO/GAUL/2015/level0")
  .filter(ee.Filter.eq("ADM0_NAME", "Hungary"));
Map.centerObject(hungary, 6);
// ========================================================
// FUNCIÓN DE EXPORTACIÓN (GeoTIFF)
// ========================================================
function exportTiff(image, name) {
  Export.image.toDrive({
    image: image,
    description: name,
    fileNamePrefix: name,
    folder: "GEE_TROPOMI_HUNGARY",
    region: hungary.geometry(),
    scale: 1000,
    crs: "EPSG:4326",
    maxPixels: 1e13
  });
}
// ========================================================
// ========================= CO ===========================
// ========================================================
function meanCO(start, end) {
  return ee.ImageCollection("COPERNICUS/S5P/OFFL/L3_CO")
    .filterDate(start, end)
    .select("CO_column_number_density")
```

```
    .mean()
    .clip(hungary);
}
var co_pre   = meanCO("2018-01-01", "2019-12-31");
var co_covid = meanCO("2020-01-01", "2020-12-31");
var co_post  = meanCO("2021-01-01", "2023-12-31");
var co_vis = {
  min: 0.02,
  max: 0.05,
  palette: ["blue", "green", "yellow", "red"]
};
Map.addLayer(co_pre,   co_vis, "CO Pre-pandemic");
Map.addLayer(co_covid, co_vis, "CO Pandemic");
Map.addLayer(co_post,  co_vis, "CO Post-pandemic");
exportTiff(co_pre,   "CO_Pre_2018_2019_Hungary");
exportTiff(co_covid, "CO_COVID_2020_Hungary");
exportTiff(co_post,  "CO_Post_2021_2023_Hungary");
// ========================================================
// ========================= NO2 ==========================
// ========================================================
function meanNO2(start, end) {
  return ee.ImageCollection("COPERNICUS/S5P/OFFL/L3_NO2")
    .filterDate(start, end)
    .select("NO2_column_number_density")
    .mean()
    .clip(hungary);
}
var no2_pre   = meanNO2("2018-01-01", "2019-12-31");
var no2_covid = meanNO2("2020-01-01", "2020-12-31");
var no2_post  = meanNO2("2021-01-01", "2023-12-31");
var no2_vis = {
```

```
  min: 0,
  max: 0.00015,
  palette: ["blue", "green", "yellow", "red"]
};
Map.addLayer(no2_pre,   no2_vis, "NO2 Pre-pandemic");
Map.addLayer(no2_covid, no2_vis, "NO2 Pandemic");
Map.addLayer(no2_post,  no2_vis, "NO2 Post-pandemic");
exportTiff(no2_pre,   "NO2_Pre_2018_2019_Hungary");
exportTiff(no2_covid, "NO2_COVID_2020_Hungary");
exportTiff(no2_post,  "NO2_Post_2021_2023_Hungary");
// ====================================================
// ======================== SO2 =======================
// ====================================================
function meanSO2(start, end) {
  return ee.ImageCollection("COPERNICUS/S5P/OFFL/L3_SO2")
    .filterDate(start, end)
    .select("SO2_column_number_density_15km")
    .mean()
    .clip(hungary);
}
var so2_pre   = meanSO2("2018-01-01", "2019-12-31");
var so2_covid = meanSO2("2020-01-01", "2020-12-31");
var so2_post  = meanSO2("2021-01-01", "2023-12-31");
var so2_vis = {
  min: 0,
  max: 0.0005,
  palette: ["blue", "green", "yellow", "red"]
};
Map.addLayer(so2_pre,   so2_vis, "SO2 Pre-pandemic");
Map.addLayer(so2_covid, so2_vis, "SO2 Pandemic");
Map.addLayer(so2_post,  so2_vis, "SO2 Post-pandemic");
```

```
exportTiff(so2_pre,   "SO2_Pre_2018_2019_Hungary");
exportTiff(so2_covid, "SO2_COVID_2020_Hungary");
exportTiff(so2_post,  "SO2_Post_2021_2023_Hungary");
```

Anex II. Seasonal Analysis (Hungary)

```
import pandas as pd
import matplotlib.pyplot as plt
from pathlib import Path
# ------------------------
# FILE PATH (same folder)
# ------------------------
DATA = Path("Hungary_air_pollution_monthly.csv")
OUT = DATA.parent  # output in same directory
# ------------------------
# LOAD DATA
# ------------------------
df = pd.read_csv(DATA, encoding="latin1")
# ------------------------
# FUNCTION: SEASONAL CYCLE
# ------------------------
def plot_seasonality(pollutant, ylabel, filename):
    tmp = (
        df[df["pollutant"] == pollutant]
        .groupby("month")["value"]
        .mean()
        .reset_index()
        .sort_values("month")
    )
    plt.figure(figsize=(8,5))
    plt.plot(
        tmp["month"],
        tmp["value"],
```

```
        linewidth=2,
        marker="o"
    )
    plt.xticks(range(1,13))
    plt.xlabel("Month")
    plt.ylabel(ylabel)
    plt.title(f"{pollutant} – Mean Monthly Cycle (Hungary)")
    plt.grid(alpha=0.3)
    plt.tight_layout()
    plt.savefig(OUT / filename, dpi=300)
    plt.close()
# ------------------------
# RUN
# ------------------------
plot_seasonality("NO₂", "NO₂ column number density (mol/m²)", "NO₂_seasonality.png")
plot_seasonality("SO₂", "SO₂ column number density (mol/m²)", "SO₂_seasonality.png")
plot_seasonality("CO", "CO column number density (mol/m²)", "CO_seasonality.png")
print("OK – Seasonal plots generated")
```

ANNEX III. City Comparison (Barplots)

```
import pandas as pd
import matplotlib.pyplot as plt
import seaborn as sns
from pathlib import Path
# ------------------------------
# FILE PATH
# ------------------------------
DATA = Path("cities_pollution.csv")
OUT = DATA.parent
# ------------------------------
# LOAD DATA
```

```
# ------------------------------
df = pd.read_csv(DATA)
df["value"] = pd.to_numeric(df["value"])
# Define period order
period_order = ["pre", "pandemic", "post"]
df["period"] = pd.Categorical(df["period"], categories=period_order, ordered=True)
# ------------------------------
# STYLE SETTINGS
# ------------------------------
plt.rcParams.update({
    "axes.titlesize": 18,
    "axes.labelsize": 14,
    "xtick.labelsize": 12,
    "ytick.labelsize": 12,
    "legend.fontsize": 12
})
sns.set_style("whitegrid")
# ------------------------------
# PLOT LOOP
# ------------------------------
for pollutant in df["pollutant"].unique():
    subset = df[df["pollutant"] == pollutant]
    plt.figure(figsize=(10,5))
    ax = sns.barplot(
        data=subset,
        x="city",
        y="value",
        hue="period",
        hue_order=period_order
    )
    plt.title(f"{pollutant} concentration by city and period")
```

```
    plt.xlabel("City")
    plt.ylabel("Column number density (mol/m²)")
    # Add labels in scientific notation
    for bar in ax.patches:
        height = bar.get_height()
        if height > 0:
            ax.text(
                bar.get_x() + bar.get_width()/2,
                height * 1.01,
                f"{height:.2e}",
                ha='center',
                va='bottom',
                fontsize=10
            )
    plt.legend(title="Period")
    plt.tight_layout()
    plt.savefig(OUT / f"{pollutant}_cities_comparison.png", dpi=300)
    plt.close()
print("OK – City comparison plots generated")
```